

# Geometric free energy of toric $\text{AdS}_4/\text{CFT}_3$ models

Sangmin Lee<sup>a,b,c,d</sup> and Daisuke Yokoyama<sup>a</sup>

<sup>a</sup>Center for Theoretical Physics, Seoul National University, R Seoul 151-747, Korea

<sup>b</sup>Department of Physics and Astronomy, Seoul National University, R Seoul 151-747, Korea

<sup>c</sup>College of Liberal Studies, Seoul National University, R Seoul 151-742, Korea

<sup>d</sup>School of Physics, Korea Institute for Advanced Study, R Seoul 130-722, Korea

E-mail: [sangmin@snu.ac.kr](mailto:sangmin@snu.ac.kr), [dd.yokoyama@gmail.com](mailto:dd.yokoyama@gmail.com)

**ABSTRACT:** We study the supersymmetric free energy of three dimensional Chern-Simons-matter theories holographically dual to  $\text{AdS}_4$  times toric Sasaki-Einstein seven-manifolds. In the large  $N$  limit, we argue that the square of the free energy can be written as a quartic polynomial of trial R-charges. The coefficients of the polynomial are determined geometrically from the toric diagrams. We present the coefficients of the quartic polynomial explicitly for generic toric diagrams with up to 6 vertices, and some particular diagrams with 8 vertices. Decomposing the trial R-charges into mesonic and baryonic variables, and eliminating the baryonic ones, we show that the quartic polynomial reproduces the inverse of the Martelli-Sparks-Yau volume function. On the gravity side, we explore the possibility of using the same quartic polynomial as the prepotential in the  $\text{AdS}$  gauged supergravity. Comparing Kaluza-Klein gravity and gauged supergravity descriptions, we find perfect agreement in the mesonic sector but some discrepancy in the baryonic sector.

**KEYWORDS:** Supersymmetry and Duality, AdS-CFT Correspondence, Chern-Simons Theories

ARXIV EPRINT: [1412.8703](https://arxiv.org/abs/1412.8703)

---

## Contents

<b>1</b>	<b>Introduction</b>	<b>1</b>
<b>2</b>	<b>Geometry</b>	<b>3</b>
2.1	Toric Sasaki-Einstein manifold	4
2.2	A-maximization revisited	5
2.3	Geometric free energy	7
2.4	5-vertex models	9
2.5	6-vertex models	10
2.6	Generalization	13
<b>3</b>	<b>Field theory</b>	<b>17</b>
3.1	Construction of field theory models	17
3.1.1	Lifting algorithm	17
3.1.2	Brane realization	18
3.1.3	Perfect matching	19
3.1.4	Computation of free energy	20
3.2	Infinite families	21
3.2.1	4 vertex models	21
3.2.2	6 vertex models	22
3.2.3	8 vertex models	26
<b>4</b>	<b>Gravity</b>	<b>29</b>
4.1	Kaluza-Klein supergravity	29
4.2	Gauged supergravity	31

---

## 1 Introduction

Branes probing toric Calabi-Yau (CY) cones offer an infinite family of AdS/CFT models with explicit AdS solutions and field theory Lagrangians. In particular, D3-branes probing a toric  $CY_3$  cone produce a  $D = 4$ ,  $\mathcal{N} = 1$  quiver gauge theory which flows to a superconformal field theory. The brane tiling model [1, 2] encodes the gauge groups, matter fields, and super-potentials of the gauge theory into a bipartite graph on a torus. Algorithms to translate between a toric diagram and the corresponding brane tiling are known.

M2-branes probing a  $CY_4$  cone similarly give rise to a  $D = 3$ ,  $\mathcal{N} = 2$  superconformal field theory. But, the problem of constructing the field theory for an arbitrary toric diagram still has not been solved completely. An M-theoretic analog of the brane tiling model, dubbed ‘brane crystal model’ [3–5], helped finding some abelian gauge theories but the non-abelian generalization was obstructed by the lack of a Lagrangian description for the

M5-brane theory. Progress was made by applying brane tiling methods to Chern-Simons-matter (CSm) theories [6–16]. The key idea is to reduce M-theory to IIA string theory along one of the  $U(1)^4$  isometry orbits. The gauge theory can be constructed in the IIA setup as usual. The information on the M-theory circle is encoded in the CS levels.

In terms of toric diagrams, the brane tiling model for M2-branes begins by projecting a three dimensional toric diagram down to two dimensions which gets uplifted back to three dimensions by the CS levels. This projection/uplifting procedure is known to work only for a limited families among all possible toric diagrams.

One of the most detailed confirmation of the toric  $AdS_5/CFT_4$  correspondence is the equivalence between  $a$ -maximization [17] and volume-minimization [18, 19], which was first proved in [20, 21]. The  $a$ -function is a cubic function of the trial R-charge which is a linear combination of all global  $U(1)$  symmetries. The coefficients of the cubic polynomial are areas of triangles in the toric diagram [22, 23]. The global symmetries have two types: mesonic and baryonic. Geometrically, mesonic symmetries are the  $U(1)^3$  isometries of the CY cone, whereas baryonic symmetries correspond to homology 3-cycles. In the proof of the equivalence [20, 21], the  $a$ -function is maximized with respect to baryonic components first. After the baryonic components are eliminated, the remaining  $a$  as a function of mesonic components is shown to be equal, up to an overall numerical factor, to the inverse of the volume [18] as a function of the Reeb vector components. The Reeb vector is the geometric counterpart of the R-charge.

The  $a$ -function is defined in terms of 't Hooft anomaly and has no counterpart in odd dimensions. For  $D = 3$ ,  $\mathcal{N} = 2$  theories, the supersymmetric free energy on three-sphere,  $F = -\log |Z_{S^3}|$ , was argued to play the role of the  $a$ -function [24–26]. Much like the  $a$ -function,  $F$  decreases along an RG flow, and the superconformal R-charge can be determined by extremizing  $F$ ; see [27] for a proof. In the large  $N$  limit, the free energy is related to the volume of the Sasaki-Einstein seven-manifold as [28–30]

$$F = N^{3/2} \sqrt{\frac{2\pi^6}{27\text{Vol}(Y_7)}}. \quad (1.1)$$

The current paper addresses the question of establishing the  $F$  vs volume relation (1.1) for arbitrary toric  $CY_4$  cone, with both sides regarded as functions of mesonic charges. Compared to the original  $a$ -max/vol-min problem, this question poses several additional difficulties. Originating from a 't Hooft anomaly, the  $a$ -function is a cubic polynomial of the coefficients of the trial R-charge. But, there is no a priori reason for the  $F$ -function to take a simple polynomial form. Even when the large  $N$  limit of the  $F$ -function takes a simple form, it is not visible until the last stage of localization computation. Computing  $F$  for many examples would be desirable. But, as mentioned earlier, there is no general method to construct the gauge theory for arbitrary toric diagram. Even when the gauge theory Lagrangian is known, some  $U(1)$  global symmetries are realized non-perturbatively and make it difficult to include in the trial R-charge with independent coefficients.

Despite these obstacles, Amariti and Franco [31] made some remarkable progress. (See [32] for an earlier attempt.) They constructed gauge theories dual to a few infinite

families of toric diagrams with up to eight vertices, and computed  $F$  in the large  $N$  limit. Trying to interpret the results in a geometric way, they argued that  $F$  should take the general form,

$$\frac{F^2}{N^3} \propto \sum_{I,J,K,L} V_{IJKL} \Delta^I \Delta^J \Delta^K \Delta^L + (\text{corrections}). \quad (1.2)$$

The  $\Delta^I$  are the coefficients of the trial R-charge, each associated to a vertex of the toric diagram, and  $V_{IJKL}$  is proportional to the volume of the tetrahedron formed by four vertices of the toric diagram. So, the leading term is a natural generalization of the cubic form of  $a$  [22, 23]. They also argued that the correction terms should be assigned to internal edges of the toric diagram. They determined the precise form of the correction term for 5-vertex models, and gave some preliminary results for 6- and 8-vertex models.

In the current paper, we propose a purely geometric method to determine the correction terms in the quartic polynomial (1.2) without restrictions from gauge theory realizations. We begin with the Amariti-Franco proposal with unknown coefficients for the correction terms. We decompose the trial R-charge into baryonic and mesonic components. Schematically, we have

$$F^2 \sim t^4 + t^3 s + t^2 s^2 + t s^3 + s^4, \quad (1.3)$$

where  $t$  and  $s$  represent baryonic and mesonic components. Our main result consists of two statements. First, the correction terms are uniquely determined by demanding that the  $t^4$  and  $t^3$  terms cancel out. Second, once the baryonic components are eliminated by extremizing  $F^2$  in (1.3), the remaining function of mesonic components coincide precisely with the inverse volume of the toric Sasaki-Einstein manifold [18, 19]. We verify our claims explicitly for most general 5- and 6-vertex models and some 8-vertex models, leaving the general case as a conjecture.

Our proposal for the geometric free energy was inspired by an analogous decoupling of baryonic charges in the  $a$ -max/vol-min problem in the  $\text{AdS}_5/\text{CFT}_4$  setup together with the concrete form of Amariti-Franco proposal for 5-vertex models. In section 2, we will review the aspects of toric geometry relevant to our problem and spell out the precise statement of our proposal. In section 3, we reproduce the field theory computation of [31] and confirm that our proposal is consistent with all infinite families of examples.

In section 4, we turn to the AdS side of  $\text{AdS}_4/\text{CFT}_3$ . In particular, we explore the possibility of using the same quartic polynomial as the prepotential in the gauged supergravity. We compute the gauge kinetic terms in Kaluza-Klein gravity and gauged supergravity descriptions. While the mesonic sector exhibits perfect agreement, the baryonic sector shows some mild discrepancy. We conclude with a comment on how to resolve the discrepancy.

## 2 Geometry

After two short reviews, we will present the geometric free energy proposal, which is the main result of the whole paper. We will give explicit form of the free energy for general 5-vertex and 6-vertex models, and close the section with a discussion on generalization.

## 2.1 Toric Sasaki-Einstein manifold

An  $n$ -dimensional toric cone  $X$  is constructed by a GLSM quotient of  $\{Z^I\} \in \mathbb{C}^d$  with respect to integer-valued charges  $Q_a^I$  ( $a = 1, \dots, d - n$ ),

$$X = \left\{ \sum_{I=1}^d Q_a^I |Z^I|^2 = 0 \right\} / (Z^I \sim e^{\theta^a Q_a^I} Z^I). \quad (2.1)$$

The cone is Calabi-Yau (CY) if and only if  $\sum_I Q_a^I = 0$  for each  $a$ .

Let  $v^i$  ( $i = 1, 2, \dots, n$ ) be the kernel of the map  $Q_a : \mathbb{Z}^d \rightarrow \mathbb{Z}^{d-n}$ , i.e.,  $Q_a^I v_I^i = 0$ . One may regard  $v_I^i$  as  $d$  lattice vectors in  $\mathbb{Z}^n$  and use them to parametrize  $|Z^I|^2 = v_I \cdot y \equiv v_I^i y_i$  ( $y \in \mathbb{R}^n$ ). The allowed values of  $y$  form a polyhedral cone  $\Delta$  defined by  $\{v_I \cdot y \geq 0\}$  in  $\mathbb{R}^n$ . The cone  $X$  is then a fibration of  $n$  angles  $\{\phi^i\}$  over the base  $\Delta$ . Using the CY condition  $\sum_I Q_a^I = 0$ , one can choose  $v_I^n = 1$  for all  $I$ , as this assignment satisfies  $Q_a^I v_I^n = 0$  automatically. With  $v_I^n = 1$ , the collection of the remaining components of  $v_I$ 's drawn on  $\mathbb{Z}^{n-1} \in \mathbb{R}^{n-1}$  will be called the toric diagram.

By construction, the toric  $X$  has  $n$  isometries  $K_i = \partial/\partial\phi^i$ . The Reeb vector  $K_R$  is in general a linear combination,  $K_R = b^i K_i$ . In [18], it was shown that the Reeb vector characterizes all the essential geometric properties of the cone  $X$ . In particular, the base  $Y$  of the cone is defined as  $Y = X \cap \{b \cdot y = 1/2\}$ . Supersymmetric cycles of  $Y$  are given by  $\Sigma^I = Y \cap \{v_I \cdot y = 0\}$ . By definition,  $X$  being Kähler or Ricci-flat is equivalent to  $Y$  being Sasakian or Einstein, respectively.

The Reeb vector determines a unique Sasakian metric on  $Y$ . The volume of  $Y$  can be computed by summing over the volume of the supersymmetric cycles  $\Sigma^I$  associated to the vertices  $v_I$  of the toric diagram. The CY condition on  $X$  fixes  $b^n = n$ . The metric of  $Y$  become Einstein at the minimum of  $\text{Vol}(Y)$  as  $(b^1, b^2, \dots, b^{n-1}; b^n = n)$  is varied inside the polyhedral cone:  $b \in \Delta$ . This is the volume-minimization to be compared with field theory results via AdS/CFT.

Concretely, for  $n = 3$ , the volume as a function of the Reeb vector is given by the Martelli-Sparks-Yau formula [18],

$$\frac{\text{Vol}_{\text{MSY}}(Y_5)}{\text{Vol}(S^5)} = \frac{1}{b^3} \sum_I \frac{\langle v_{I-1}, v_I, v_{I+1} \rangle}{\langle b, v_{I-1}, v_I \rangle \langle b, v_I, v_{I+1} \rangle} \equiv \frac{1}{b^3} \sum_I L^I(b). \quad (2.2)$$

Here,  $\langle u, v, w \rangle$  denotes the determinant of the  $(3 \times 3)$  matrix made out of vectors  $u, v, w$ . For  $n = 4$ , the volume is again expressed as a sum over the vertices of the toric diagram,

$$\frac{\text{Vol}_{\text{MSY}}(Y_7)}{\text{Vol}(S^7)} = \frac{1}{b^4} \sum_I L^I(b), \quad (2.3)$$

but the precise form of  $L^I(b)$  depends on how many neighboring vertices the vertex  $v_I$  has. In the simplest case of three nearest neighbors, say,  $\{v_J, v_K, v_L\}$ , it is given by

$$L^I(b) = M_{JKL}^I(b) \equiv \frac{\langle v_I, v_J, v_K, v_L \rangle^2}{\langle b, v_I, v_J, v_K \rangle \langle b, v_I, v_K, v_L \rangle \langle b, v_I, v_L, v_J \rangle}. \quad (2.4)$$

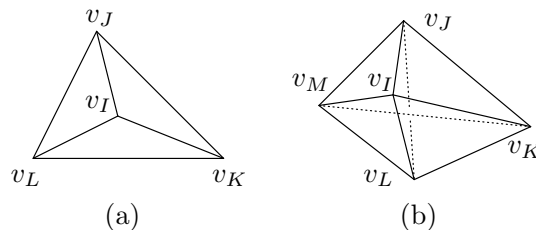


**Figure 1.** The volume of the supersymmetric cycle associated to a vertex  $v_I$ . When viewed from the “outside” of the toric diagram, the neighboring vertices  $\{v_J, v_K, \dots\}$  are aligned along the “polygon” in a clock-wise order. (a) Three neighboring vertices introduce a tetrahedron (b) Four neighboring vertices lead to a triangulation composed of two tetrahedra

Our convention for the orientation of the vertices are explained in figure 1. When there are more than three neighboring vertices, we can triangulate the “polygon” composed of neighboring vertices to compute  $L^I$ . For instance, with four neighboring vertices, we obtain

$$L^I = M_{JKL}^I + M_{JLM}^I = M_{JKM}^I + M_{MKL}^I. \quad (2.5)$$

The generalization to more neighboring vertices is straightforward.

As explained in [33], when  $Y$  is simply-connected, which we assume for the rest of this paper, the homology group of  $Y$  is given by  $H_{2n-3}(Y, \mathbb{Z}) = \mathbb{Z}^{d-n}$ . If  $C^a$  ( $a = 1, \dots, d-n$ ) form a basis of  $(2n-3)$ -cycles of  $Y$ , it can be shown that  $\Sigma^I = Q_a^I C^a$  with  $Q_a^I$  being precisely the GLSM data (2.1). As the harmonic  $(2n-3)$ -forms  $\omega_a$  dual to  $C^a$  measure the baryonic charges of  $\Sigma^I$ , we have

$$B_a[\Sigma^I] = \int_{\Sigma^I} \omega_a = Q_a^I. \quad (2.6)$$

As one can see from the torus action in the GLSM description (2.1), for simply connected  $Y$ , the baryonic charges  $Q_a^I$  and the mesonic charges ( $K_i = \partial/\partial\phi^i$ ) together span  $\mathbb{Z}^d$ . This means that the toric relation  $Q_a^I v_I^i = 0$  can be extended to

$$\begin{pmatrix} Q_a^I \\ F_i^I \end{pmatrix} \begin{pmatrix} u_I^b \\ v_I^j \end{pmatrix} = \begin{pmatrix} \delta_a^b & 0 \\ 0 & \delta_i^j \end{pmatrix}, \quad (2.7)$$

for some integer-valued matrices  $F_i^I$  and  $u_I^b$  [23].

The volume of a supersymmetric cycle is mapped to the superconformal R-charge of the corresponding local operator via AdS/CFT [34]. For later convenience, we follow [18] to define the geometric R-charge  $\Delta_{\text{MSY}}^I(b)$  as

$$\Delta_{\text{MSY}}^I(b) = \frac{2L^I(b)}{\sum_I L^I(b)}. \quad (2.8)$$

## 2.2 A-maximization revisited

For toric theories, the  $a$ -function takes a simple geometric form [22, 23]

$$\bar{a}(\Delta) \equiv \frac{a(\Delta)}{N^2} = \frac{9}{32} C_{IJK} \Delta^I \Delta^J \Delta^K = \frac{9}{64} |\langle v_I, v_J, v_K \rangle| \Delta^I \Delta^J \Delta^K, \quad (2.9)$$

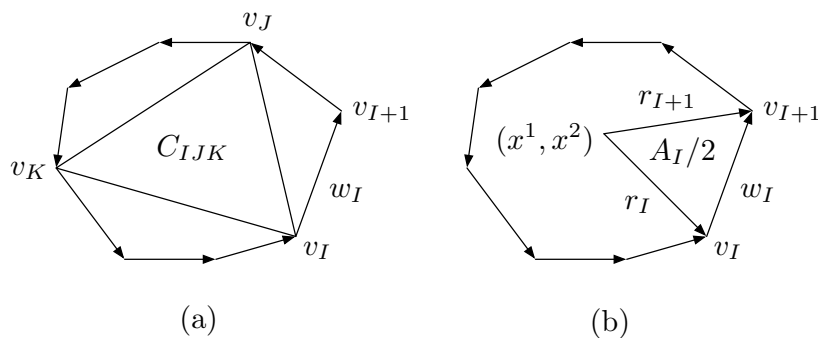


**Figure 2.** Toric diagram of  $CY_3$ .

where each coefficient

$$C_{IJK} = \frac{1}{2} |\langle v_I, v_J, v_K \rangle| \quad (2.10)$$

is the area of the triangle composed of three vertices  $(I, J, K)$  on the toric diagram.

**Volume as the inverse of  $a$ : overview.** The equivalence between  $a$ -maximization and volume-minimization was originally proved in [20]. The proof was simplified in [23] using the triangle formula (2.10). The proof roughly consists of three steps.

First, we decompose the trial R-charges into a linear combination of the baryonic and the mesonic charges,

$$\Delta^I = t^a Q_a^I + s^i F_i^I. \quad (2.11)$$

In terms of the  $t$  and  $s$  variables, the  $a$ -function decomposes into, schematically,

$$a \sim t^3 + t^2 s + t s^2 + s^3. \quad (2.12)$$

Second, by mathematical induction using (2.10) [22, 23], we can show that the  $t^3$  terms vanish identically for any toric theory. The remaining terms can be reorganized as

$$a = -m_{ab}(s) t^a t^b + 2n_a(s) t^a + R(s), \quad (2.13)$$

where  $m_{ab}$ ,  $n_a$ ,  $R$  are homogeneous polynomials of degree one, two and three in  $s$ , respectively. Extremizing  $a$  with respect to  $t$ , we obtain an intermediate result,

$$\Delta^I(s) = Q_a^I m^{ab}(s) n_b(s) + s^i F_i^I, \quad \bar{a}(s) = R(s) + m^{ab}(s) n_a(s) n_b(s), \quad (2.14)$$

where  $m^{ab}$  is the matrix inverse of  $m_{ab}(s)$ .

Finally, the equivalence between  $a$ -maximization and volume-minimization is established by proving that

$$\Delta^I(s) = \Delta_{\text{MSY}}^I(b) \big|_{s=(2/3)b}, \quad \bar{a}(s) = \frac{\pi^3}{4\text{Vol}_{\text{MSY}}(b)} \bigg|_{s=(2/3)b}. \quad (2.15)$$

**Some details.** We review parts of the proof of the assertions above that will be relevant for generalizations to the  $\text{AdS}_4/\text{CFT}_3$  setting. To begin with, for general  $\text{CY}_n$ , we define the normalized Reeb vector  $x^i$  by

$$x^i = \frac{s^i}{2} = \frac{b^i}{n} \quad (i = 1, \dots, n), \quad (2.16)$$

such that  $x^n = 1$  and the domain of  $x^{i=1, \dots, n-1}$  is precisely the interior of the toric diagram. We rewrite the relation (2.2), (2.3) between  $\text{Vol}(Y)$  and  $\text{Vol}(\Sigma^I)$  as

$$S(x) = \frac{1}{x^n} \sum_I L^I(x), \quad (2.17)$$

As shown in [18], it is a part of a more general relation,

$$\sum L^I(x) v_I^i = \frac{x^i}{x^n} \sum_I L^I(x) = x^i S(x), \quad (2.18)$$

which can be proved by applying Stokes' theorem in the toric diagram.

Specializing to  $\text{CY}_3$ , with  $(b^1, b^2, b^3) = 3(x^1, x^2, x^3 = 1)$ , we introduce [23]

$$\begin{aligned} r_I &= (v_I^1, v_I^2) - (x^1, x^2), & w_I &= (v_{I+1}^1, v_{I+1}^2) - (v_I^1, v_I^2), \\ A_I &= \langle r_I, w_I \rangle \equiv \det \begin{pmatrix} r_I^1 & r_I^2 \\ w_I^1 & w_I^2 \end{pmatrix}, & L^I(x) &= \frac{\langle w_{I-1}, w_I \rangle}{A_{I-1} A_I}, & S(x) &= \frac{1}{x^3} \sum_I L^I(x). \end{aligned} \quad (2.19)$$

See figure 2(b) for the geometric meaning of each quantity.

Now, the first half of the proof of (2.15) asserts that the baryon charges decouple from the maximization process:

$$\text{Tr} B R^2|_{\Delta_{\text{MSY}}^I} = 0 \quad \text{or equivalently} \quad C_{IJK} B^I L^J L^K = 0. \quad (2.20)$$

The other half states that

$$a_{\text{CFT}}|_{\Delta_{\text{MSY}}^I} = \frac{\pi^3}{4 \text{Vol}_{\text{MSY}}} \quad \text{or equivalently} \quad C_{IJK} L^I L^J L^K = 3S^2. \quad (2.21)$$

As proved in [22, 23], both (2.20) and (2.21) follow from a single lemma:

$$c_I \equiv C_{IJK} L^J L^K = 3S + \langle r_I, u \rangle, \quad (2.22)$$

where  $u$  is some vector independent of the label  $I$ . Once the lemma is proved, (2.20) follows from  $\sum_I Q_a^I = 0 = \sum_I Q_a^I v_I$  and (2.21) from  $\sum_I L^I r_I = 0$ .

### 2.3 Geometric free energy

Amariti and Franco [31] computed the large  $N$  free energy of a large class of toric  $\text{CFT}_3$ 's. They found that, for all examples they considered, the following relation holds:

$$\bar{F}^2(\Delta) \equiv \frac{9F^2(\Delta)}{2\pi^2 N^3} = \frac{2}{3} C_{IJKL} \Delta^I \Delta^J \Delta^K \Delta^L, \quad (2.23)$$



where the coefficients take the general form,

$$C_{IJKL} = |\langle v_I, v_J, v_K, v_L \rangle| + (\text{corrections}). \quad (2.24)$$

The normalization for  $\bar{F}^2$  is chosen such that  $\bar{F}^2 = 1$  for  $\text{CY}_4 = \mathbb{C}^4$ .

We warn the readers that the “correction” terms are not meant to be smaller than the “leading” terms. They are just less obvious than the leading terms. Amariti and Franco also noticed that all correction terms are somehow associated to internal lines of the toric diagram. More specifically, there is a type 1 correction term for each internal line, and a type 2 correction term for each pair of internal lines.

The goal of this section is to turn the observations of Amariti and Franco to a general conjecture for the form of correction terms and to gain some geometric understanding. As an application of the conjecture, we will determine the correction terms explicitly for generic toric diagrams with 5 or 6 vertices and some specific diagrams with 7 or 8 vertices.

The key idea behind the conjecture is that the correction terms Amariti and Franco found for particular examples are such that the quartic and cubic terms in baryonic components of the trial R-charge (to be called  $t^4$  and  $t^3$  terms below) vanish identically. We reverse the logic and base our conjecture on four central assumptions.

1. The leading term always take the same form as in (2.24).
2. The type 1 and type 2 terms explained below (2.24) exhaust all possible corrections.
3. The coefficients of the correction terms are rational functions of  $|\langle v_I, v_J, v_K, v_L \rangle|$ .
4. The vanishing of  $t^4$  and  $t^3$  constrains the correction coefficients.

The decoupling of baryonic charges goes in close parallel with the  $\text{AdS}_5/\text{CFT}_4$  story reviewed in the previous subsection. We decompose the trial R-charges as

$$\Delta^I = t^a Q_a^I + s^i F_i^I. \quad (2.25)$$

The charges are subject to  $\sum_I \Delta^I = 2$ , which is equivalent to  $s^4 = 2$  and  $b^4 = 4$ . It is a special case of (2.16) at  $n = 4$ . In terms of the  $t$  and  $s$  variables, the function  $F^2$  looks like

$$F^2 \sim t^4 + t^3 s + t^2 s^2 + t s^3 + s^4. \quad (2.26)$$

Our conjecture propose that the correction terms should be chosen such that the  $t^4$  and  $t^3$  terms vanish. A priori, the existence and the uniqueness of such correction terms are not obvious at all. At the time of writing, we do not know how to prove or disprove the conjecture. We will simply explore the possibilities by starting from the simplest case and proceeding to more complicated ones.

Assuming the vanishing of  $t^4$  and  $t^3$  terms in (2.26), we can organize the remaining terms as follows,

$$F^2 = -m_{ab}(s)t^a t^b + 2n_a(s)t^a + R(s). \quad (2.27)$$

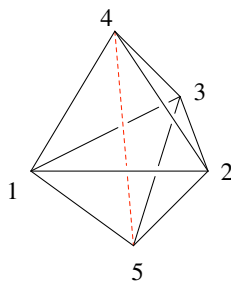


**Figure 3.** A generic toric diagram with 5 vertices has one internal line.

The functions  $m_{ab}$ ,  $n_a$  and  $R$  are homogeneous polynomials of  $s$  of degree 2, 3 and 4, respectively. Maximizing  $F^2$  with respect to  $t$  gives  $t^a = m^{ab}n_b$ . Inserting it back to (2.25) and (2.27), we obtain

$$\begin{aligned}\bar{\Delta}^I(s) &= Q_a^I m^{ab}(s) n_b(s) + s^i F_i^I, \\ \bar{F}^2(s) &= R(s) + m^{ab}(s) n_a(s) n_b(s).\end{aligned}\tag{2.28}$$

Further extremization of  $\bar{F}^2$  determines the “vacuum” value of  $s$ , which we call  $s_*$ .

A major sequel to our conjecture is that  $\bar{\Delta}^I$  and  $\bar{F}^2$  match their geometric counterparts even before extremization with respect to  $s$ , just as in the proof [20] of the  $a$ -maximization vs volume-minimization.

$$\Delta^I(s) = \Delta_{\text{MSY}}^I(b) \big|_{s=b/2}, \quad \bar{F}^2(s) = \frac{\pi^4}{3\text{Vol}_{\text{MSY}}(b)} \bigg|_{s=b/2}.\tag{2.29}$$

Again, it is not clear how this result follows from our conjecture. In the following subsections, we will verify this claim for several families of concrete examples and sketch some ideas for the general proof.

## 2.4 5-vertex models

As shown in figure 3, a generic toric diagram with 5 vertices contains one internal line. The non-generic configuration with no internal line can be smoothly reached from the generic case. For instance, one can move the vertex 4 in figure 3 continuously, with all others fixed, until the internal line  $\overline{45}$  intersects the external edge  $\overline{12}$ .

The Amariti-Franco proposal [31] for the 5-vertex model is

$$\bar{F}^2(\Delta) = \sum_{I < J < K < L} V_{IJKL} \Delta^I \Delta^J \Delta^K \Delta^L - \frac{V_{1245} V_{2345} V_{3145}}{V_{1234} V_{1235}} (\Delta^4 \Delta^5)^2,\tag{2.30}$$

where we defined  $V_{IJKL} = |\langle v_I, v_J, v_K, v_L \rangle|$ . This proposal is the simplest non-trivial case of our general conjecture. The simplicity of the 5-vertex model allows us to prove the vanishing of  $t^4$  and  $t^3$  terms by straightforward computation.

**Vanishing of  $t^4$  and  $t^3$  terms.** Taking account of the relative orientations of the vertices, one can remove the absolute value sign from the definition of  $V_{IJKL}$ ,

$$\begin{aligned}V_{1234} &= -\langle v_1, v_2, v_3, v_4 \rangle, & V_{1235} &= +\langle v_1, v_2, v_3, v_5 \rangle, \\ V_{1245} &= \langle v_1, v_2, v_4, v_5 \rangle, & V_{2345} &= \langle v_2, v_3, v_4, v_5 \rangle, & V_{3145} &= \langle v_3, v_1, v_4, v_5 \rangle,\end{aligned}\tag{2.31}$$

The 5-vertex models have only one set of GLSM charges  $Q_{a=1}^I \equiv Q^I$ . One may define

$$(I, J, K, L) \equiv \langle v_I Q^I, v_J Q^J, v_K Q^K, v_L Q^L \rangle \quad (\text{no sum over indices}). \quad (2.32)$$

Using the fact that  $\sum_I v_I Q^I = 0$ , one can replace all  $(I, J, K, L)$ 's by, say,  $(1, 2, 3, 4)$ :

$$(1, 2, 3, 5) = -(1, 2, 3, 4), \quad (2, 3, 4, 5) = -(2, 3, 4, 1) = +(1, 2, 3, 4). \quad (2.33)$$

Now, the coefficient of the  $t^4$  term,  $C_{IJKL} Q^I Q^J Q^K Q^L$ , is proportional to

$$\begin{aligned} & -(1234) + (1235) + (1245) + (2345) + (3145) + \frac{(1245)(2345)(3145)}{(1234)(1235)} \\ &= \{-1 - 1 + 1 + 1 + 1\}(1, 2, 3, 4) - \frac{(1, 2, 3, 4)^3}{(1, 2, 3, 4)^2} = 0. \end{aligned} \quad (2.34)$$

Next, the coefficients of  $t^3$  terms are proportional to  $T_I \equiv C_{IJKL} Q^J Q^K Q^L$ .  $T_1$  is proportional to

$$\begin{aligned} & -(1, 2, 3, 4) + (1, 2, 3, 5) + (1, 2, 4, 5) + (3, 1, 4, 5) \\ &= \{-1 - 1 + 1 + 1\}(1, 2, 3, 4) = 0, \end{aligned} \quad (2.35)$$

and similarly for  $T_2$  and  $T_3$ . On the other hand,  $T_4$  is proportional to

$$\begin{aligned} & -(1234) + (1245) + (2345) + (3145) + 2 \frac{(1245)(2345)(3145)}{(1234)(1235)} \\ &= \{-1 + 1 + 1 + 1\}(1, 2, 3, 4) - 2 \frac{(1, 2, 3, 4)^3}{(1, 2, 3, 4)^2} = 0, \end{aligned} \quad (2.36)$$

and similarly for  $T_5$ . This completes the proof of the vanishing of all  $t^4$  and  $t^3$  terms for general 5-vertex models.

**Volume as the inverse of  $F^2$ .** For general 5-vertex models, it is straightforward, albeit tedious, to integrate out the  $t$  variable and prove the identity (2.29) relating  $\bar{F}^2(s)$  to the inverse of  $\text{Vol}_{\text{MSY}}(b)$ . In practice, the algebraic manipulation is most easily done with the aid of a computer program.

## 2.5 6-vertex models

The Amariti-Franco proposal [31] does not cover all generic 6-vertex models. As explained earlier, we use the vanishing of  $t^4$  and  $t^3$  terms to find the form of the correction terms. Under the general assumptions of our conjecture, the correction terms are uniquely determined. Moreover, once the  $t$  variables are integrated out, the resulting  $\bar{F}^2(s)$  is shown to be proportional to  $\text{Vol}_{\text{MSY}}(b)$  as in (2.29).

The computation involves quite a few variables. The position of the 6 vertices in  $\mathbb{R}^3$  are specified by 18 parameters. Using the homogeneity of  $F^2$  as well as the  $\text{SL}(3, \mathbb{Z})$  and translation symmetries of the toric diagram, we can fix 12, leaving 6 free parameters. The Reeb vector components add 3 variables. Proving identities among rational functions of 9 variables is often impractical even with a computer program. We use the well-known

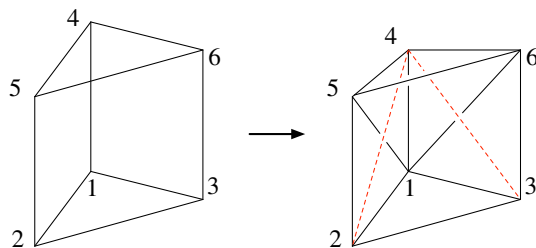


**Figure 4.** A toric diagram with 6 vertices and two internal lines emanating from the same vertex.

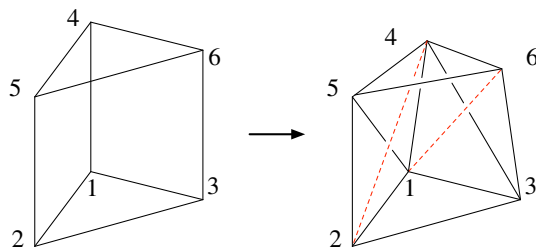


**Figure 5.** A toric diagram with 6 vertices and two non-intersecting internal lines.

fact that two rational functions are identical to each other if they yield the same value at sufficiently many different “sampling” points. The number of points should be greater than the sum of degrees of the numerator and the denominator of the rational function. Throughout this subsection, it should be understood that the vanishing of  $t^4$ ,  $t^3$  terms and the equivalence between  $\bar{F}^2$  and  $\text{Vol}_{\text{MSY}}$  have been verified by the sampling method.

The 6-vertex models have a number of distinct configurations of internal lines. One way to proceed is to begin with a toric diagram with no internal line and to add internal lines one at a time by deforming the position of some of the vertices.

**Two internal lines meeting at a vertex.** One such example is depicted in figure 4. We begin with a ‘triangular prism’ which has no internal line. By pushing the vertex 4 toward the edge  $\overline{56}$ , we introduce two internal lines  $\overline{24}$  and  $\overline{34}$ .

After some trial and error in numerical experiment, we find the two types of corrections terms:

$$\begin{aligned}\delta_1(F^2) &= -\frac{V_{2456}V_{2461}V_{2415}}{V_{2561}V_{4561}}(\Delta^2\Delta^4)^2 - \frac{V_{3465}V_{3451}V_{3416}}{V_{3561}V_{4561}}(\Delta^3\Delta^4)^2, \\ \delta_2(F^2) &= -2\frac{V_{2415}V_{3461}}{V_{4561}}\left(\frac{V_{4abc}}{V_{1abc}}\right)(\Delta^2\Delta^4)(\Delta^3\Delta^4).\end{aligned}\tag{2.37}$$

Here, the indices  $abc$  are three elements from  $\{2, 3, 5, 6\}$ . The choice of which three elements does not affect the result since the four vertices  $\{v_2, v_3, v_5, v_6\}$  lie on the same plane.

**Two internal lines not meeting each other.** Another example with two internal lines is depicted in figure 5. We begin again with the triangular prism and push the vertex 4 slightly parallel to the edge  $\overline{56}$ .

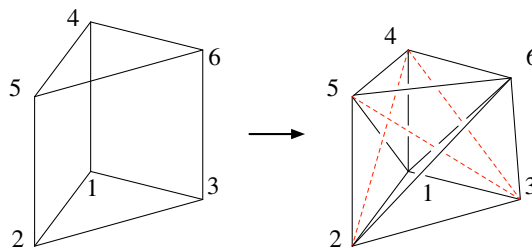


**Figure 6.** A toric diagram with 6 vertices and three internal lines connected at vertices.

The correction terms in this case are

$$\begin{aligned}\delta_1(F^2) &= -\frac{V_{2453}V_{2431}V_{2415}}{V_{2531}V_{4531}}(\Delta^2\Delta^4)^2 - \frac{V_{1634}V_{1645}V_{1653}}{V_{1345}V_{6345}}(\Delta^1\Delta^6)^2, \\ \delta_2(F^2) &= 2\frac{V_{2415}V_{3461}}{V_{1345}}(\Delta^2\Delta^4)(\Delta^1\Delta^6).\end{aligned}\quad (2.38)$$

This example meets the previous one when the vertices  $\{v_1, v_3, v_4, v_6\}$  fall onto the same plane such that  $V_{3461} = 0$ . The coefficients of the  $(\Delta^2\Delta^4)^2$  term in (2.37) and (2.38) look different, but they can be shown to be equal when  $\{v_1, v_3, v_4, v_6\}$  lie on the same plane.

**Three connected internal lines.** We deform figure 4 further by turning on the third internal line  $\overline{35}$ . The result is depicted in figure 6.

The correction terms turn out to be

$$\begin{aligned}\delta_1(F^2) &= -\frac{V_{2456}V_{2461}V_{2415}}{V_{2561}V_{4561}}(\Delta^2\Delta^4)^2 - \frac{V_{5321}V_{5316}V_{2356}}{V_{2561}V_{2361}}(\Delta^3\Delta^5)^2 \\ &\quad - (1-R)\frac{V_{2346}V_{1345}V_{3461}}{V_{1236}V_{1456}}(\Delta^3\Delta^4)^2, \\ \delta_2(F^2) &= -2\frac{V_{2415}V_{3461}V_{4256}}{V_{4561}V_{1256}}(\Delta^2\Delta^4)(\Delta^3\Delta^4) - 2\frac{V_{2356}V_{3461}V_{3125}}{V_{1236}V_{6125}}(\Delta^3\Delta^4)(\Delta^3\Delta^5) \\ &\quad + 2\frac{V_{1245}V_{2356}}{V_{1256}}(\Delta^2\Delta^4)(\Delta^3\Delta^5).\end{aligned}\quad (2.39)$$

Here,  $R$  denotes the ratio of products of volumes,

$$R = \frac{V_{1245}V_{2356}V_{3164}}{V_{3145}V_{1256}V_{2364}}, \quad (2.40)$$

which is non-zero only when all three internal lines are turned on.

**Three disconnected internal lines.** We deform figure 5 further by turning on the third internal line  $\overline{35}$ . The result is depicted in figure 7.

The correction terms turn out to be

$$\begin{aligned}\delta_1(F^2) &= -\frac{1}{1+R}\left(\frac{V_{4256}}{V_{1256}}\frac{V_{2134}}{V_{5134}}V_{2415}(\Delta^2\Delta^4)^2 + (\text{cyclic})\right), \\ \delta_{2A}(F^2) &= \frac{2}{1+R}\left(\frac{V_{1245}V_{3164}}{V_{3145}}(\Delta^2\Delta^4)(\Delta^1\Delta^6) + (\text{cyclic})\right), \\ \delta_{2B}(F^2) &= -\frac{2R}{1+R}\left(V_{2416}(\Delta^2\Delta^4)(\Delta^1\Delta^6) + (\text{cyclic})\right),\end{aligned}\quad (2.41)$$

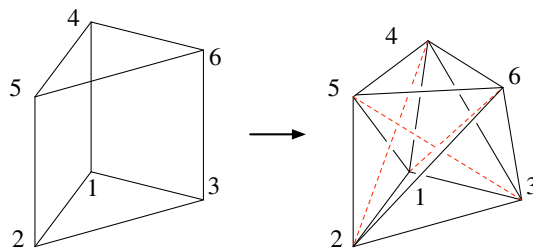


**Figure 7.** A toric diagram with 6 vertices and three non-intersecting internal lines.

where  $R$  is as defined in (2.40) and “+(cyclic)” means a sum over the cyclic permutations,

$$(123; 456) \rightarrow (231; 564) \rightarrow (312; 645) \rightarrow (123; 456). \quad (2.42)$$

In the limit where  $\overline{35}$  disappears,  $R$  vanishes and  $\delta_1$  and  $\delta_{2A}$  reproduce (2.38). To make the comparison, aside from reshuffling some indices, we need to use some identities that hold when  $\{v_2, v_3, v_5, v_6\}$  are coplanar. The new term,  $\delta_{2B}$ , is visible only if all three internal lines are turned on.

As a further check for (2.41), we can take the limit where all three internal lines meet at a point, as is the case for the example (A.4) of [31]. In that limit,  $\delta_{2B}$  vanishes again, not because  $R = 0$  but because  $V_{2416}$  and its cyclic permutations vanish. For the particular example (A.4) of [31], it turns out that  $R = 1$  and (2.41) reproduces eq. (A.5) of [31] including the precise normalization.<sup>1</sup>

Note that while (2.41) agrees with eq. (A.5) of [31] numerically for arbitrary choices of the variables  $\{X_{1,2}, Y_{1,2}, Z_{1,2}\}$ , our geometric interpretation for the coefficients of the correction terms differs from one suggested by [31]. For instance, the coefficient of the  $(\Delta^2 \Delta^4)^2$  term in (2.41) is

$$-\frac{V_{4256}V_{2134}V_{2415}}{(1+R)V_{1256}V_{5134}} = -\frac{V_{4256}V_{2134}V_{2415}V_{2364}}{V_{1245}V_{2356}V_{3164} + V_{3145}V_{1256}V_{2364}}. \quad (2.43)$$

In contrast, eq. (6.8) of [31] suggests an interpretation of the form

$$-\frac{V_a V_b V_c + V_b V_c V_d + V_c V_d V_a + V_d V_a V_b}{V_e V_f}, \quad (2.44)$$

which appears quite different from (2.43).

## 2.6 Generalization

**Some 7-vertex and 8-vertex models.** Conceptually, our strategy to find the correction terms can be applied to toric diagrams with arbitrary number of vertices. However, the brute force computation becomes intractable as early as at 7-vertex, even with the aid of a computer. To collect more evidence for our conjecture while keeping the computational complexity under control, we explored a few non-generic 7-vertex and 8-vertex models. Two such examples are depicted in figure 8. In all examples we considered, the correction terms were uniquely determined, in accordance with our conjecture.

<sup>1</sup>Caution: there is an overall factor of 4 difference between our normalization and that of [31].

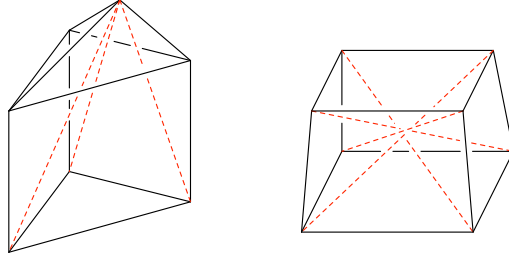


**Figure 8.** Some non-generic toric diagrams with 7 or 8 vertices.

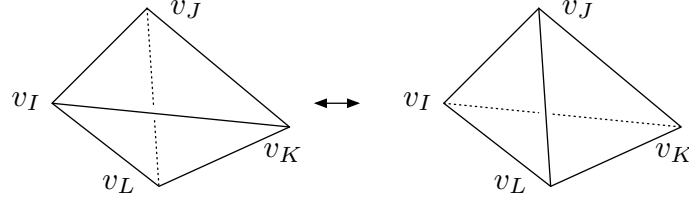


**Figure 9.** A “flop” transition.

We have not been able to derive a more systematic way to determine the correction terms. In the rest of this subsection, we sketch some ideas which may prove useful in future attempts to find new systematic methods.

**Flop transition.** Consider a generic toric diagram with  $d$  vertices. By “generic”, we mean that the boundary surface of the convex polytope can be decomposed into triangles such that no two triangles lie on the same plane. It is easy to show that

$$\#(\text{external edges}) = 3d - 6, \quad \#(\text{internal edges}) = \frac{(d-3)(d-4)}{2}. \quad (2.45)$$

Recall that all the correction terms of the geometric free energy formula were associated to internal lines. As we deform the toric diagram continuously, the form of the correction terms remain unchanged until a “crossing” occurs. By “crossing”, we mean the crossing of an internal line with an external edge. Whenever a crossing occurs, a pair of neighboring triangles go through a “flop” transition as depicted in figure 9.

It seems reasonable to assume that the terms in  $F^2$  that are completely independent of the four vertices involved in the flop transition will remain unchanged. At least, this assumption is consistent with all explicit results we have obtained up to 8-vertex models. The terms that will change can be organized as follows:

$$\begin{aligned} \text{Type 0.} \quad & V_{IJKL} \Delta^I \Delta^J \Delta^K \Delta^L, \\ \text{Type 1(a).} \quad & (\Delta^I \Delta^K)^2, \quad (\Delta^J \Delta^L)^2, \\ \text{Type 1(b).} \quad & (\Delta^I \Delta^A)^2, \quad (\Delta^J \Delta^A)^2, \quad (\Delta^K \Delta^A)^2, \quad (\Delta^L \Delta^A)^2, \\ \text{Type 2(a).} \quad & (\Delta^I \Delta^K)(\Delta^A \Delta^B), \quad (\Delta^J \Delta^L)(\Delta^A \Delta^B), \\ \text{Type 2(b).} \quad & (\Delta^I \Delta^A)(\Delta^J \Delta^B), \quad (\Delta^J \Delta^A)(\Delta^K \Delta^B), \quad (\Delta^K \Delta^A)(\Delta^L \Delta^B), \\ & (\Delta^L \Delta^A)(\Delta^I \Delta^B), \quad (\Delta^I \Delta^A)(\Delta^K \Delta^B), \quad (\Delta^J \Delta^A)(\Delta^L \Delta^B), \end{aligned} \quad (2.46)$$

where the the vertices  $v_A, v_B$  does not belong to  $\{v_I, v_J, v_K, v_L\}$ .

We may take the following approach to determine the coefficients of the correction terms. (1) Assume that we have some value of  $C_{IJKL}$  such that  $t^3$  and  $t^4$  terms vanish. (2) When going through the “flop”, we know how the Type 0 term changes. (3) We could try to determine how other terms should change in order to maintain the vanishing of  $t^3$  and  $t^4$  terms. Some preliminary studies indicate that, although this approach gives rise to a set of constraints on the unknown coefficients, the constraints are not sufficient by themselves to determine all coefficients completely.

**Recursive approach.** In a recursive approach, after finishing the study of toric diagrams with  $d$  vertices, we may add a new “ $(d+1)$ -th” vertex and see how things change:

$$v_I^i \rightarrow \tilde{v}_I^i = \left( \frac{v_I^i}{v_{d+1}^i} \right). \quad (2.47)$$

To proceed, we need the GLSM charge matrix for the new toric diagram whose rank should be  $(d+1) - n$ . We will use the following recursive construction:

$$Q_a^I \rightarrow \tilde{Q}_a^I = \left( \frac{Q_a^I}{v_{d+1}^i F_i^I} \middle| \begin{array}{c} 0 \\ -1 \end{array} \right). \quad (2.48)$$

Generically, the new vertex produces  $(d-3)$  extra internal lines. Since the  $t^4$ ,  $t^3$  terms from all the pre-existing vertices cancel out among themselves, the same cancellation should occur among the additional leading and correction terms.

**Some geometric identities.** We want to see how much information from section 2.2 can be carried over to the current setup. Recall from (2.18) that

$$\sum L^I(x) v_I^i = \frac{x^i}{x^4} \sum_I L^I(x) = x^i S(x), \quad (2.49)$$

where  $x^i$  is the normalized Reeb vector and  $L^I$  and  $S$  are defined in 2.1. For  $i \neq 4$ , the identity can be understood as a consequence of the following relation,

$$L^I r_I = \sum_{J \in N_I} c^{IJ} w_{IJ} \quad (c^{IJ} = c^{JI}, w_{IJ} = -w_{JI}). \quad (2.50)$$

Here,  $J \in N_I$  means that vertices  $J$  and  $I$  are neighbors sharing an external edge. The explicit form of the coefficients is known

$$w_{IJ} = v_I - v_J, \quad c^{IJ} = \frac{V_{IJKL}}{\langle x, v_I, v_J, v_K \rangle \langle x, v_I, v_J, v_L \rangle}, \quad (2.51)$$

with  $J, K$  being the vertices of the two triangles meeting over the edge  $\overline{IJ}$ ; see figure 10.

In the CY<sub>3</sub> setup reviewed in section 2.2, there was an interesting identity (2.22):

$$C_{IJK} L^J L^K = \frac{3S}{x^3} + \langle v_I, x, u \rangle \implies C_{IJK} L^I L^J L^K = 3S^2|_{x^3=1}. \quad (2.52)$$



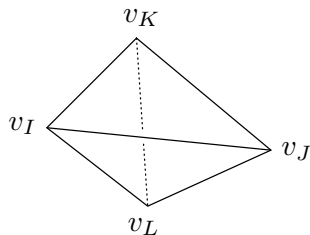


**Figure 10.** The formula for  $c^{IJ}$ .

where the vector  $u$  is independent of the vertex label  $I$ . We propose that a  $CY_4$  analog of (2.52) may hold, namely,

$$c_I \equiv C_{IJKL} L^J L^K L^L = \frac{4S^2}{x^4} + \langle v_I, x, u \rangle \implies C_{IJKL} L^I L^J L^K L^L = 4S^3|_{x^4=1}. \quad (2.53)$$

for some “two-form”  $u$ . We content ourselves with verifying the proposal (2.53) for 5-vertex models, leaving a more general analysis for a future work.

We set  $x^4 = 1$  and define  $r_I^i = v_I^i - x^i$  such that a  $(4 \times 4)$  determinant can be rewritten as a  $(3 \times 3)$  determinant

$$\langle v_I, v_J, v_K, x \rangle \equiv \begin{vmatrix} v_I^1 & v_I^2 & v_I^3 & 1 \\ v_J^1 & v_J^2 & v_J^3 & 1 \\ v_K^1 & v_K^2 & v_K^3 & 1 \\ x^1 & x^2 & x^3 & 1 \end{vmatrix} = \begin{vmatrix} r_I^1 & r_I^2 & r_I^3 \\ r_J^1 & r_J^2 & r_J^3 \\ r_K^1 & r_K^2 & r_K^3 \end{vmatrix} \equiv \langle r_I, r_J, r_K \rangle \quad (2.54)$$

Similarly, for a “two-form”  $u$  with vanishing components along the  $x^4$  direction, we may write  $\langle v_I, x, u \rangle = \langle r_I, u \rangle$ . We further abbreviate  $\langle r_I, r_J, r_K \rangle$  as  $\langle I, J, K \rangle$  in what follows.

After some manipulations, it is possible to show that

$$\begin{aligned} c_1 &= -S(\langle 1, 2, 4 \rangle L^2 L^4 + \langle 1, 3, 5 \rangle L^3 L^5), \\ c_2 &= -S(\langle 2, 3, 4 \rangle L^3 L^4 + \langle 2, 1, 5 \rangle L^1 L^5), \\ c_3 &= -S(\langle 3, 1, 4 \rangle L^1 L^4 + \langle 3, 2, 5 \rangle L^2 L^5). \end{aligned} \quad (2.55)$$

Combining this fact with a particular choice of basis for  $u$ ,

$$u = -\frac{S}{\langle 1, 2, 3 \rangle} (a_1 r_2 \wedge r_3 + a_2 r_3 \wedge r_1 + a_3 r_1 \wedge r_2), \quad (2.56)$$

we obtain an exact expression for  $u$  with

$$\begin{aligned} a_1 &= \langle 1, 2, 4 \rangle L^2 L^4 + \langle 1, 3, 5 \rangle L^3 L^5 + 4S, \\ a_2 &= \langle 2, 3, 4 \rangle L^3 L^4 + \langle 2, 1, 5 \rangle L^1 L^5 + 4S, \\ a_3 &= \langle 3, 1, 4 \rangle L^1 L^4 + \langle 3, 2, 5 \rangle L^2 L^5 + 4S. \end{aligned} \quad (2.57)$$

Another lengthy but straightforward computation verifies the identity  $c_I = 4S^2 + \langle r_I, u \rangle$  for the remaining  $I = 4, 5$ . This expression for  $u$  is fairly simple and exhibits the symmetries  $(1 \rightarrow 2 \rightarrow 3 \rightarrow 1, 4 \leftrightarrow 5)$ , but the generalization to more vertices does not seem obvious.

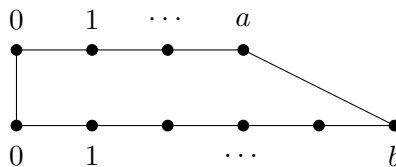


**Figure 11.** Toric diagram for  $L^{a,b,a}$ . We assume  $b \geq a$  without loss of generality.

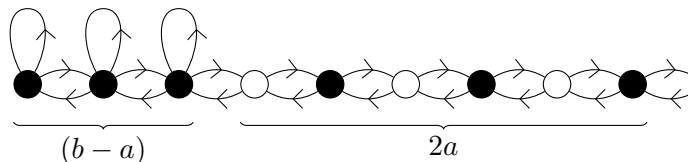


**Figure 12.** Quiver diagram for  $L^{a,b,a}$  model. This diagram is for  $a = 3$ ,  $b = 6$ . This is originally a circular diagram. We cut it and place it on a line, keeping in mind that the right end and the left end should be identified.

### 3 Field theory

In this section, we review the field theory computation performed in [31]. We first review the general method of constructing field theory models and of computing the free energy in the large  $N$  limit. Then we examine a few infinite families of field theories considered in [31]. By comparing the field theory result and their geometric counterpart, we verify that all the results of [31] agree perfectly with our main conjecture.

#### 3.1 Construction of field theory models

##### 3.1.1 Lifting algorithm

We restrict our attention to 3d toric CS theories that have some 4d “parent” theory. In particular, we will take the  $L^{a,b,a}$  geometry for the parent theory.

We will use an algorithm for uplifting this toric diagram to three dimensions, which correspond to the 3d CS theory. The uplifting algorithm to be used in this paper is a special case of a more general method discussed in [9, 10, 14–16]. In the toric diagram, we assign an integer  $Q_\alpha$  ( $\alpha = 1, \dots, a$ ) to each vertex on the upper row except the leftmost one. Similarly, we assign an integer  $P_\beta$  ( $\beta = 1, \dots, b$ ) to each vertex on the lower row except the leftmost one. We also assign a degeneracy to each vertex. The  $\mu$ -th vertex on the upper row has degeneracy  ${}_a C_\mu$ , and the  $\nu$ -th vertex on the lower row has degeneracy  ${}_b C_\nu$ . The degenerate points on each vertex move in the “vertical” direction as follows.

Let us focus on the upper row. The “elevation” of each of the  ${}_a C_\mu$  degenerate points is equal to the partial sum of  $\mu$  elements taken from the set  $\{Q_\alpha\}$ . For example, consider

$$Q_\alpha = (0, 1, 0, 2) \quad (a = 4), \quad (3.1)$$

and  $\mu = 2$  as illustrated in figure 13. There are  ${}_4 C_2 = 6$  pairs of  $Q_\alpha$ . The partial sums are

$$\begin{aligned} Q_1 + Q_2 = 1, \quad Q_1 + Q_3 = 0, \quad Q_1 + Q_4 = 2, \\ Q_2 + Q_3 = 1, \quad Q_2 + Q_4 = 3, \quad Q_3 + Q_4 = 2. \end{aligned} \quad (3.2)$$

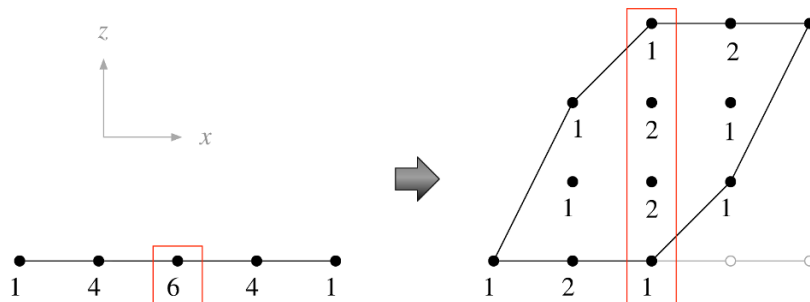


**Figure 13.** Uplifting degenerate points for  $Q_\alpha = (0, 1, 0, 2)$ .

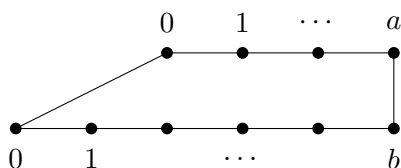


**Figure 14.** Flipped toric diagram for  $L^{a,b,a}$ .

Thus, among the  ${}_4C_2 = 6$  degenerate points, one stays at the bottom, two move up one step, two move up two steps, and one moves up three steps. The same manipulation should be done for all points in the upper row as well as those in the lower row, producing the 3d toric diagram.

The 3d gauge theory has the same gauge groups and matter fields as its parent theory. What change the vacuum moduli space from  $CY_3$  to  $CY_4$  are the CS terms. To determine the CS levels, we align  $Q_\alpha$  and  $P_\beta$  in a particular order to define  $p_i$  ( $i = 1, \dots, a + b$ )

$$p_i = (P_1, P_2, P_3, Q_1, P_4, Q_2, P_5, Q_3, P_6). \quad (a = 3, b = 6 \text{ example}) \quad (3.3)$$

and determine the level  $k_i$  as the differences in  $p_i$ ,

$$k_i = p_i - p_{i-1} \quad (3.4)$$

We may reorder the integers  $Q_\alpha$  and/or  $P_\beta$  but it will not affect the large  $N$  free energy [31]. This is consistent with the uplifting algorithm to construct the 3d toric diagram discussed above, which is clearly independent of the reordering.

**Flip symmetry.** By an  $SL(3, \mathbb{Z})$  transformation, the toric diagram of an  $L^{a,b,a}$  model in figure 11 can be transformed to a flipped form in figure 14. The flip reveals a slightly hidden left-right (in the  $x$ -direction) symmetry of the toric diagram, which will give a restriction on the critical value of the Reeb vector components. The flip symmetry may or may not survive the uplifting procedure depending on the assignment of  $Q_\alpha$ ,  $P_\beta$ . The 3d toric diagram may also have some additional symmetries.

### 3.1.2 Brane realization

We explain how to determine the CS terms for the  $L^{a,b,a}$  models from a brane configuration of the ABJM type [35]. As illustrated in figure 15, when a NS5-brane and  $k$  D5-branes

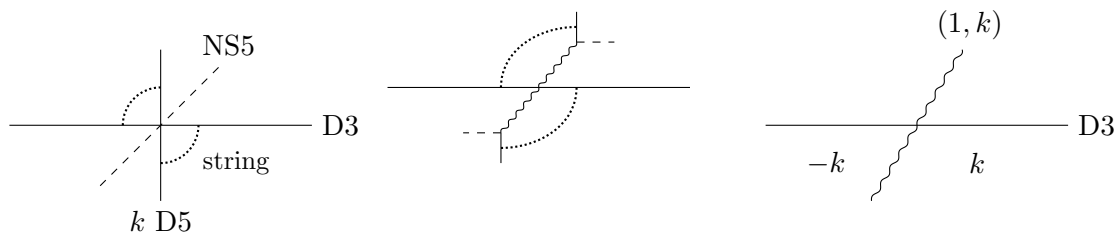


**Figure 15.** CS term from brane configuration.

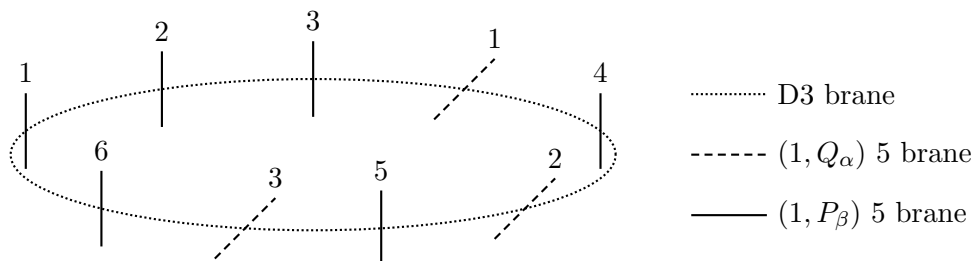


**Figure 16.** Brane configuration of  $L^{a,b,a}$  model ( $a = 3$ ,  $b = 6$ ).

merge to produce a  $(1, k)$  brane, the string connecting D3 and D5 branes become massive. As the massive state is integrated out, a fermion loop generates a CS term. Due to the relative orientation, the CS level for the left and right neighboring D3-brane is  $k$  and  $-k$ , respectively.

The brane figuration for the  $L^{a,b,a}$  model is depicted in figure 16. Each stack of  $N$  D3-branes between two neighboring 5-branes gives rise to a  $U(N)$  gauge group. The strings connecting two sides of a 5-brane produce (anti-)bifundamental fields. When two consecutive 5-branes are of the same type  $(1, P_\beta)$ , the gauge group in the middle hosts an adjoint field as well. Thus the gauge theory can be summarized by the quiver diagram in figure 12. The brane realization also explains why the CS levels for the gauge theory are given by (3.4).

### 3.1.3 Perfect matching

Perfect matching maps each vertex of the toric diagram, including degenerate ones, to a global symmetry of the CS theory. External perfect matchings, those associated to non-degenerate external vertices, carry non-vanishing trial R-charges.

For  $L^{a,b,a}$  models, the vertices on the upper row of the toric diagram in figure 11 correspond to the bi-fundamental and adjoint fields attached to the right side of white circles in figure 12. The vertices on the lower row correspond to the bi-fundamentals attached to the right side of black dots. The detailed map between the degenerate vertices and the matter fields are as follows. Again, let us focus on the upper row first. There are  $\sum_{\mu=0}^a a C_\mu = 2^a$  vertices in the upper row. Each vertex corresponds to a global charge. On the other hand, there are  $a$  white circles in figure 12, and each white circle has a pair of bifundamental fields (left-pointing and right-pointing ones) on the right. Let us take one bifundamental field from each pair. There are  $2^a$  possible choices. Among those,

there are  ${}_a C_\mu$  ways to choose  $\mu$  left-pointing bifundamental fields and  $(a - \mu)$  right-pointing bifundamental fields from the  $a$  pairs. The selected bifundamental fields and all the adjoint fields have a unit charge for a global symmetry related to the  $\mu$ -th vertex, and  ${}_a C_\mu$  ways of the selection corresponds to the degeneracy. Similarly, on the lower row, the  $\nu$ -th vertices corresponds to  ${}_b C_\nu$  global symmetries for which  $\nu$  left-pointing bifundamental fields and  $(b - \nu)$  right-pointing bifundamental fields from the  $b$  pairs to the right of the black dots (but no adjoint field) have a unit charge.

There is a slightly different but equivalent explanation. When we uplift a 2d toric diagram, we considered the combinations of  $\{Q_\alpha\}$ . For the bifundamental fields, we can also consider the combinations of left-pointing and right-pointing fields. For the upper row, pairs of bifundamental fields (left-pointing and right-pointing ones) to the right of the white circle in figure 12 are relevant. For the degenerate vertices at the  $\mu$ -th point, we picked  $\mu$  out of  $a$   $\{Q_\alpha\}$  charges. Similarly, we pick  $\mu$  out of  $a$  left-pointing bifundamental fields and  $(a - \mu)$  right-pointing bifundamental fields from the  $a$  pairs. Then, the selected bifundamental fields as well as all the adjoint fields have a unit charge for a global symmetry. The specified global symmetry in this procedure corresponds to the shifted vertex by the choice of  $\{Q_\alpha\}$  charges. Even after the shift, some of the vertices are still degenerate. The residual degeneracy will not affect later discussions, since the trial R-charges are associated to external, non-degenerate vertices only. For the lower row, we do the same procedure for the bifundamentals to the right of the black dots. The only difference from the upper row is that the adjoint fields are not included.

### 3.1.4 Computation of free energy

The method to calculate the large  $N$  free energy for a vector-like theory is well explained in, e.g., [36]. Here, we only give a minimal summary of the procedure, mainly to establish our notation. The supersymmetric localization method reduces a path integral to a finite dimensional integral over the eigenvalues of some scalar fields. In the large  $N$  limit, the eigenvalues are described approximately by a continuous distribution. In the end, the large  $N$  free energy can be expressed in terms of integrals over the eigenvalue distribution.

$$F_{\text{CS}}^i = \frac{N^{3/2}}{2\pi} \int x \rho(x) k_i y_i dx, \quad (3.5)$$

$$F_{\text{adj}}^i = \frac{2N^{3/2}}{3} \pi^2 \Delta_i (1 - \Delta_i) (2 - \Delta_i) \int \rho^2 dx, \quad (3.6)$$

$$F_{\text{bi}}^{i,j} = -N^{3/2} \frac{2 - \Delta_{ij}^+}{2} b \int \rho^2 dx \left\{ \left( y_i - y_j + \pi \Delta_{ij}^- \right)^2 - \frac{\pi^2}{3} \Delta_{ij}^+ (4 - \Delta_{ij}^+) \right\}. \quad (3.7)$$

Here,  $x$  is the real part of the normalized eigenvalue,  $y$  is the imaginary part, and  $\rho(x)$  is the eigenvalue density. The first contribution comes from the CS terms of  $U(N)_i$  gauge groups, the second from adjoint fields, and the last from a pair of bifundamental fields.  $\Delta_i$  are the R-charges of adjoint fields, and  $\Delta_{ij}^+$  and  $\Delta_{ij}^-$  are the sum and difference of R-charges of a pair of bifundamental fields between gauge groups  $U(N)_i$  and  $U(N)_j$ . The free energy

for the  $L^{a,b,a}$  model is given by

$$F_{aba} = \sum_{i=1}^{a+b} F_{\text{CS}}^i + \sum_{i=1}^{b-a} F_{\text{adj}}^i + \sum_{i=1}^{a+b} F_{\text{bi}}^{i,i+1}, \quad (3.8)$$

where  $a + b + 1 = 1 \pmod{a+b}$  is understood. Note that this expression only depends on  $\delta y_i = y_i - y_{i+1}$ ;  $\sum_i k_i y_i = \sum_i \delta y_i p_i$  where  $p_i$  are ones defined in (3.3). The final expression can be derived by minimizing this expression in terms of  $\rho$  and  $\delta y_i$ 's subject to three constraints:

$$\int \rho(x) dx = 1, \quad \sum_i \delta y_i = 0, \quad |\delta y_i + \pi \Delta_i^-| \leq \pi \Delta_i^+. \quad (3.9)$$

## 3.2 Infinite families

In this subsection, we will reproduce a few infinite series of examples from [31] with slight changes of notations to facilitate the comparison with other sections in the present paper. In each example, we begin with the assignment of  $(Q_\alpha, P_\beta)$  and construct the toric diagram using the uplifting algorithm. We use the  $\text{SL}(4, \mathbb{Z})$  freedom to put the toric diagram in a frame where the symmetries of the diagram become manifest. We will mostly focus on the  $k = 1$  case. General value of  $k$  can be reached by taking a  $\mathbb{Z}_k$  orbifold of the  $k = 1$  case.

The goal of this subsection is to verify that the field theory results from [31] agree with our geometric free energy. Precisely how the comparison is made, however, requires some explanation. In all but the simplest examples to be considered, turning on all possible trial R-charge components make the field theory computation unwieldily complex. Fortunately, all the toric diagrams have enough symmetry to reduce the number of free component of trial R-charge to one. We will denote the free component by  $\Delta$  without any indices. The precise map between  $\Delta$  and the Reeb vector components can be deduced from MSY volume formulas. Once the consistency between the field theory result and the MSY formula is fully verified, it remains to show that our geometric free energy also agrees with the MSY formula. The latter connection is stronger since we can keep all three components of the Reeb vector  $(b^1, b^2, b^3; b^4 = 4)$  as free parameters.

### 3.2.1 4 vertex models

We consider the assignment,  $Q_\alpha = 0$ ,  $P_\beta = k$ . The CS level is determined by (3.4),

$$\vec{k} = (0, \dots, 0 \mid -k, k, \dots, -k, k). \quad (3.10)$$

The 3d toric diagram obtained by the uplifting method is depicted in figure 17(a). In what follows, we will use the diagram in figure 17(b) related to the original one by an  $\text{SL}(4, \mathbb{Z})$  transformation.

In the field theory computation of the free energy [31], it is possible to turn on all four components of the trial R-charge. Each components are mapped to external perfect matchings on the toric diagram. The result, taken from [31], is

$$\bar{F}_{\text{ft}}^2 = 16ab\Delta^1\Delta^2\Delta^3\Delta^4. \quad (3.11)$$

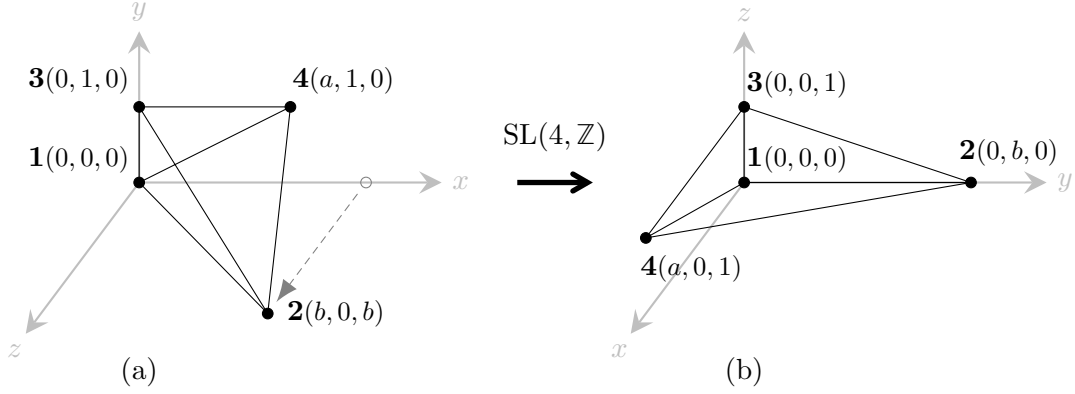


**Figure 17.** 4 vertex model.

The subscript “ft” stands for field theory. The agreement with our geometric formula is obvious:  $\bar{F}_{\text{ft}}^2 = \bar{F}_{\text{geo}}^2$ . The comparison with the MSY formula is also straightforward. The MSY volume formula gives

$$Z_{\text{MSY}} = \frac{\text{Vol}(S^7)}{\text{Vol}_{\text{MSY}}(b)} = \frac{ab}{b^1 b^2 (b^1 - ab^3) (b^2 + b(b^3 - b^4))}. \quad (3.12)$$

The geometric values for the R-charge components are

$$\Delta_{\text{MSY}}^1 = -\frac{b^2 + b(b^3 - b^4)}{2b}, \quad \Delta_{\text{MSY}}^2 = \frac{b^2}{2b}, \quad \Delta_{\text{MSY}}^3 = -\frac{b^1 - ab^3}{2a}, \quad \Delta_{\text{MSY}}^4 = \frac{b^1}{2a}. \quad (3.13)$$

In terms of the R-charge components, the MSY volume takes the orbifold form

$$Z_{\text{MSY}} = \frac{1}{16ab(\Delta^1 \Delta^2 \Delta^3 \Delta^4)_{\text{MSY}}}. \quad (3.14)$$

Thus, we find  $\bar{F}^2 = Z_{\text{MSY}}^{-1}$  as expected.

For later convenience, let us illustrate how the flip symmetry of the 3d toric diagram reduces free components of the R-charge. The geometric R-charges for those external vertices exchanged by the flip symmetry should be equated: ( $b^4 = 4$ )

$$\Delta^1 = \Delta^2 \implies 2b^2 = b(b^3 - 4), \quad \Delta^3 = \Delta^4 \implies 2b^1 = ab^3. \quad (3.15)$$

Note that the vertices **3** and **4** are flipped along the  $x$ -direction and **1** and **2** are flipped along the  $y$ -direction. Each flip gives information of a corresponding component of the Reeb vector. Now we can parametrize the volume in terms of one parameter, say,  $b^3 = 4\Delta$ :

$$b^1 = 2a\Delta, \quad b^2 = 2b(1 - \Delta), \quad b^3 = 4\Delta, \quad b^4 = 4, \quad (3.16)$$

$$\Delta_{\text{MSY}}^1 = \Delta_{\text{MSY}}^2 = 1 - \Delta, \quad \Delta_{\text{MSY}}^3 = \Delta_{\text{MSY}}^4 = \Delta, \quad (3.17)$$

$$Z_{\text{MSY}} = \frac{1}{16ab\Delta^2(1 - \Delta)^2}. \quad (3.18)$$

### 3.2.2 6 vertex models

In all 6-vertex and 8-vertex models to be considered below, we will use the symmetry of the toric diagrams to reduce the number of free parameters in the Reeb vector to one from the very beginning.

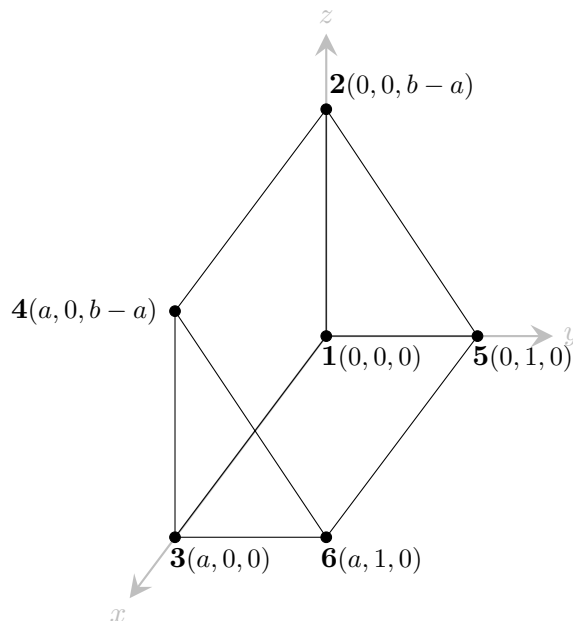


**Figure 18.** 6 vertex model, Family 1.

**Family 1.** Consider the  $(P, Q)$  charges

$$Q_\alpha = \underbrace{(k, \dots, k)}_a, \quad P_\beta = \underbrace{(0, \dots, 0)}_{b-a} \underbrace{(k, \dots, k)}_a \quad (3.19)$$

The CS level is determined by (3.4),

$$\vec{k} = (-k, 0, \dots, 0 \mid k, 0, \dots, 0) \quad (3.20)$$

The 3d toric diagram, with labels and coordinates of the vertices, is depicted in figure 18.

The field theory computation in [31], with only one free parameter in the trial R-charge turned on, gave

$$\bar{F}_{\text{ft}}^2 = a(b-a)\Delta(1-\Delta)^2. \quad (3.21)$$

On the geometry side, the MSY volume formula gives

$$Z_{\text{MSY}} = \frac{a(b-a)b^4}{b^1 b^2 b^3 (b^1 - ab^4)((b-a)b^2 + b^3 + (a-b)b^4)}. \quad (3.22)$$

The geometric R-charges are<sup>2</sup>

$$\Delta^1 = -\frac{(b^1 - ab^4)((b-a)b^2 + b^3 + (a-b)b^4)}{a(a-b)b^4}, \quad (3.23)$$

$$\Delta^2 = \frac{b^3(b^1 - ab^4)}{a(a-b)b^4}, \quad \Delta^3 = \frac{b^1((b-a)b^2 + b^3 + (a-b)b^4)}{a(a-b)b^4}, \quad (3.24)$$

$$\Delta^4 = -\frac{b^1 b^3}{a(a-b)b^4}, \quad \Delta^5 = -\frac{b^2(b^1 - ab^4)}{ab^4}, \quad \Delta^6 = \frac{b^1 b^2}{ab^4}. \quad (3.25)$$

---

<sup>2</sup>To avoid clutter, we omit the subscript MSY when the meaning is clear from the context.



Again, we set  $b^4 = 4$  and impose the flip symmetry. The flip along  $x$ -direction exchanges **1** and **3**, **2** and **4**, and **5** and **6**. The  $x$ -flip determines the value of  $b^1$ ,

$$\Delta^1 = \Delta^3, \quad \Delta^2 = \Delta^4, \quad \Delta^5 = \Delta^6 \implies b^1 = 2a. \quad (3.26)$$

Similarly, the  $z$ -flip symmetry solves  $b^3$  for other parameters.

$$\Delta^1 = \Delta^2, \quad \Delta^3 = \Delta^4 \implies b^3 = \frac{1}{2}(b-a)(4-b^2). \quad (3.27)$$

The field theory result and the geometric result can be identified if we relabel  $b^2 = 4\Delta$ . Other variables depend on  $\Delta$  as

$$b^1 = 2a, \quad b^2 = 4\Delta, \quad b^3 = 2(b-a)(1-\Delta), \quad b^4 = 4, \quad (3.28)$$

$$\Delta^1 = \Delta^2 = \Delta^3 = \Delta^4 = \frac{1}{2}(1-\Delta), \quad \Delta^5 = \Delta^6 = 2\Delta. \quad (3.29)$$

Inserting these into the MSY volume formula, we find

$$Z_{\text{MSY}} = \frac{1}{16a(b-a)\Delta(1-\Delta)^2} = (\bar{F}_{\text{ft}}^2)^{-1}. \quad (3.30)$$

It is straightforward to compare these results with the main conjecture of section 2. For this particular family, the toric diagram contains no genuine internal line, the free energy receives no correction term. The geometric free energy is

$$\begin{aligned} \bar{F}^2 = & \Delta^1 \Delta^2 \Delta^5 (\Delta^3 + \Delta^4 + \Delta^6) + \Delta^3 \Delta^4 \Delta^6 (\Delta^1 + \Delta^2 + \Delta^5) \\ & + \Delta^1 \Delta^2 \Delta^6 (\Delta^3 + \Delta^4) + \Delta^2 \Delta^3 \Delta^5 (\Delta^4 + \Delta^6) + \Delta^1 \Delta^4 \Delta^5 (\Delta^3 + \Delta^6). \end{aligned} \quad (3.31)$$

Decomposing  $\Delta^I$  into mesonic and baryonic variables as in (2.11) and integrating out the baryonic ones, we get  $\bar{F}^2 = Z_{\text{MSY}}^{-1}$  with  $b^i = 2s^i$ .

**Family 2.** We set  $b = 2a$  for simplicity. The  $(P, Q)$  data are

$$Q_\alpha = (\underbrace{k, \dots, k}_a), \quad P_\beta = (\underbrace{0, \dots, 0}_a, \underbrace{2k, \dots, 2k}_a). \quad (3.32)$$

The CS level is determined by (3.4),

$$\vec{k} = (-2k, 0, \dots, 0 \mid k, k, -k, k, -k, \dots, k, -k, k). \quad (3.33)$$

The 3d toric diagram, with labels and coordinates of the vertices, is depicted in figure 19.

The volume and geometric R-charges are given by

$$\begin{aligned} Z_{\text{MSY}} &= \frac{2aA}{b^1 BCDEFG}, \\ \Delta^1 &= \frac{BCDE}{aA}, & \Delta^2 &= -\frac{BCb^1(2ab^1 + 3ab^4 - b^2)}{A}, \\ \Delta^3 &= -\frac{FGb^1(ab^1 + ab^4 + b^2)}{A}, \\ \Delta^4 &= \frac{CEG(ab^1 + 2ab^4 - 2b^3)}{2aA}, & \Delta^5 &= \frac{BDF(ab^1 + 2ab^4 + 2b^3)}{2aA}, \\ \Delta^6 &= \frac{DEFG}{aA}, \end{aligned} \quad (3.34)$$

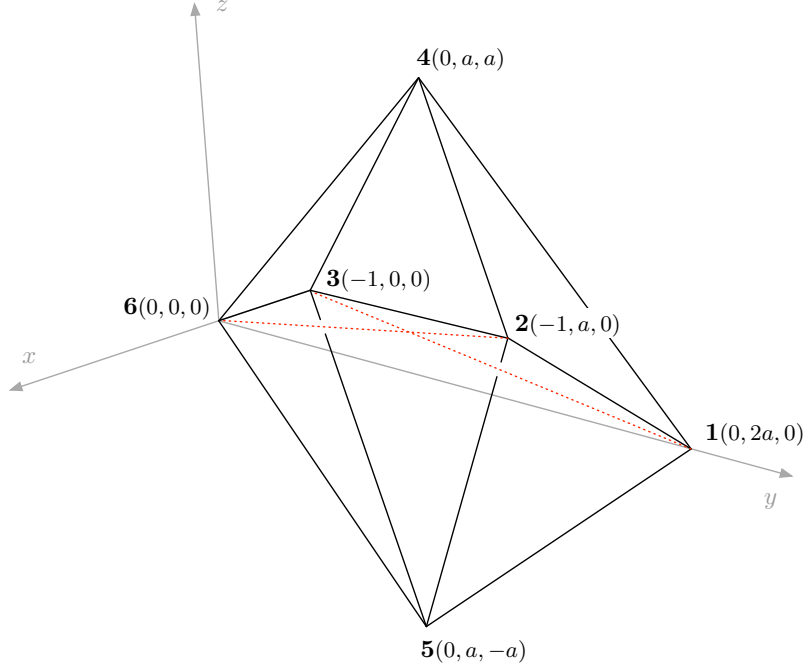


**Figure 19.** 6 vertex model, Family 2.

where we introduced some short-hand notations,

$$\begin{aligned}
 A &= a(a^2b_1^3 + 5a^2b_1^2b_4 + 8a^2b_1b_4^2 + 4a^2b_4^3 - ab_1^2b_2 - 2ab_1b_2b_4 + b_1b_2^2 - 3b_1b_3^2 - 4b_3^2b_4) \\
 B &= (b^2 - b^3), \quad C = (b^2 + b^3), \quad D = (a(b^1 + b^4) - b^3), \\
 E &= (a(b^1 + b^4) + b^3), \quad F = (ab^1 + 2ab^4 - b^2 - b^3), \quad G = (ab^1 + 2ab^4 - b^2 + b^3). \quad (3.35)
 \end{aligned}$$

The  $z$ -flip symmetry, which identifies vertices **4** and **5**, demands that  $b^3 = 0$ . The  $y$ -flip symmetry, which follows from the 2d toric diagram of the parent theory, implies

$$\Delta^1 = \Delta^6 \implies b^2 = \frac{a}{2}(b^1 + 8), \quad (3.36)$$

$$\Delta^2 = \Delta^3 \implies b^2 = \frac{a}{2}(b^1 + 8) \quad (\text{less trivial}). \quad (3.37)$$

Here and later, less trivial means that there are multiple solutions to the equation. However, the requirement that the Reeb vector should lie inside the toric diagram rules out the extra unphysical solution.

Relabeling  $b^1 = -4\Delta$ , we rewrite the Reeb vector and the trial R-charges as

$$b^1 = -4\Delta, \quad b^2 = 2a(2 - \Delta), \quad b^3 = 0, \quad b^4 = 4, \quad (3.38)$$

$$\Delta^1 = \Delta^6 = \frac{4(1 - \Delta)^2}{4 - 3\Delta}, \quad \Delta^2 = \Delta^3 = 2\Delta, \quad \Delta^4 = \Delta^5 = \frac{2(1 - \Delta)(2 - \Delta)}{4 - 3\Delta}. \quad (3.39)$$

The MSY volume formula gives

$$Z_{\text{MSY}} = \frac{4 - 3\Delta}{32a^2\Delta(1 - \Delta)^2(2 - \Delta)^2}. \quad (3.40)$$

This coincides with the inverse of  $\bar{F}_{\text{ft}}^2$  computed from the field theory [31].

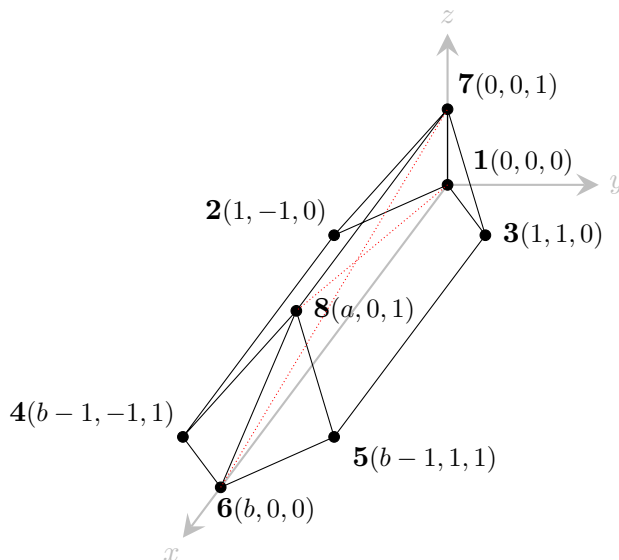


**Figure 20.** 8 vertex model, Family 1.

We can test our main conjecture on this example. The internal lines of the toric diagram give rise to non-trivial corrections. Applying the methods of section 2, we find

$$\delta_1 = -\frac{a^2}{2} ((\Delta^1 \Delta^3)^2 + (\Delta^2 \Delta^6)^2), \quad \delta_2 = +a^2 \Delta^1 \Delta^3 \Delta^2 \Delta^6. \quad (3.41)$$

Including the correction terms and integrating out the baryonic variables, we again confirm  $\bar{F}^2 = Z_{\text{MSY}}^{-1}$ .

### 3.2.3 8 vertex models

**Family 1.** The  $(P, Q)$  charges are

$$Q_\alpha = (\underbrace{k, \dots, k}_a), \quad P_\beta = (0, \underbrace{k, \dots, k}_{b-2}, 2k). \quad (3.42)$$

The CS level is determined by (3.4):

$$\vec{k} = (-2k, k, 0, \dots, 0 \mid 0, \dots, 0, k) \quad (3.43)$$

The 3d toric diagram is depicted in figure 20.

We use the  $y$ -flip symmetry of the toric diagram to set  $b^2 = 0$ . We also impose the  $x$ -flip symmetry:

$$\Delta^1 = \Delta^6, \quad \Delta^7 = \Delta^8 \text{ (less trivial)} \implies b^1 = \frac{1}{2}(4b + (a-b)b^3). \quad (3.44)$$

Relabeling  $b^3 = 4\Delta$ , we rewrite the Reeb vector and the trial R-charges as

$$\begin{aligned} b^1 &= 2(b + (a - b)\Delta), & b^2 &= 0, & b^3 &= 4\Delta, & b^4 &= 4, \\ \Delta^1 &= \Delta^6 = \frac{4(1 - \Delta)^2}{(2 + b)(1 - \Delta) + a\Delta}, & \Delta^7 &= \Delta^8 = 2\Delta, \\ \Delta^2 &= \Delta^3 = \Delta^4 = \Delta^5 = -\frac{(1 - \Delta)(b(1 - \Delta) + a\Delta)}{(2 + b)(1 - \Delta) + a\Delta}. \end{aligned} \quad (3.45)$$

The MSY volume formula gives

$$Z_{\text{MSY}} = \frac{(2 + b)(1 - \Delta) + a\Delta}{32\Delta(1 - \Delta)^2(b(1 - \Delta) + a\Delta)^2}. \quad (3.46)$$

It agrees with the field theory computation of [31] with the same parametrization in  $\Delta$ .

We do not have a general form of the correction terms for arbitrary 8-vertex models. But, from the number of internal lines and the symmetries of the toric diagram, we know that the correction terms have only two independent coefficients. Demanding that the  $t^4$  and  $t^3$  terms vanish as we did in section 2, we can determine the correction terms uniquely:

$$\delta_1 = -\frac{a}{2} ((\Delta^1 \Delta^8)^2 + (\Delta^6 \Delta^7)^2), \quad \delta_2 = +a\Delta^1 \Delta^6 \Delta^7 \Delta^8. \quad (3.47)$$

Upon eliminating baryonic charges and imposing the same symmetries for the mesonic charges, we recover the same result for the volume (3.46).

**Family 2.** The  $(P, Q)$  charges are

$$Q_\alpha = (\underbrace{0, \dots, 0}_Y, \underbrace{k, \dots, k}_{a-Y}), \quad P_\beta = (\underbrace{0, \dots, 0}_X, \underbrace{k, \dots, k}_{b-X}). \quad (3.48)$$

Here,  $X$  and  $Y$  are integers satisfying  $0 < X < b$ ,  $0 < Y < a$ . The CS level can be determined by (3.4), but its form depends on the values of  $a, b, X, Y$ .

- $b - X > a$

$$\begin{aligned} \vec{k} &= (-k_1, 0, \dots, 0, k_{X+1}, 0, \dots, 0, \\ &\quad -k_{b-a+1}, k_{b-a+2}, \dots, -k_{b-a+2Y-1}, k_{b-a+2Y}, 0, \dots, 0) \end{aligned} \quad (3.49)$$

- $a \geq b - X > a - Y$

$$\begin{aligned} \vec{k} &= (-k_1, 0, \dots, 0, k_{a-b+2X+2}, -k_{a-b+2X+3}, \\ &\quad k_{a-b+2X+4}, \dots, -k_{b-a+2Y-1}, k_{b-a+2Y}, 0, \dots, 0) \end{aligned} \quad (3.50)$$

- $a - Y \geq b - X$

$$\begin{aligned} \vec{k} &= (-k_1, 0, \dots, 0, k_{b-a+2Y+1}, -k_{b-a+2Y+2}, \\ &\quad k_{b-a+2Y+3}, \dots, -k_{a-b+2X}, k_{a-b+2X+1}, 0, \dots, 0) \end{aligned} \quad (3.51)$$

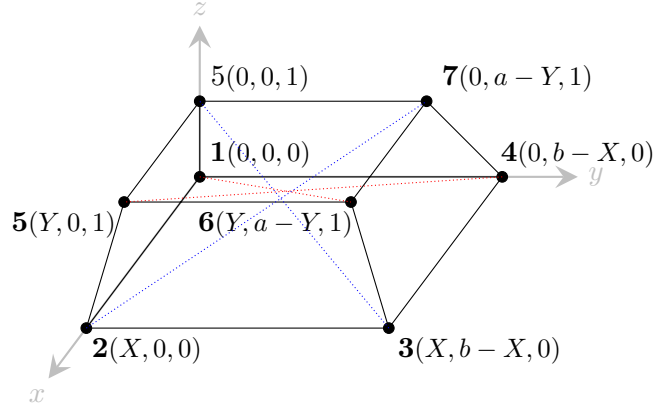


**Figure 21.** 8 vertex model, Family 2.

where  $k_i = k$  and the subscript  $i$  refers to the positions of the non-vanishing entries.

The 3d toric diagram is depicted in figure 21. We introduce the parametrization  $b^3 = 4\Delta$  from the outset and impose the  $x$ - and  $y$ -flip symmetries:

$$\Delta^1 = \Delta^2 \quad : \quad b^1 = 2(X(1 - \Delta) + Y\Delta), \quad (3.52)$$

$$\Delta^1 = \Delta^4 \quad : \quad b^2 = 2((b - X)(1 - \Delta) + (a - Y)\Delta), \quad (3.53)$$

The geometric R-charges take a simple form,

$$\Delta^1 = \Delta^2 = \Delta^3 = \Delta^4 = 1 - \Delta, \quad \Delta^5 = \Delta^6 = \Delta^7 = \Delta^8 = \Delta. \quad (3.54)$$

The MSY volume formula gives

$$Z_{\text{MSY}} = \frac{1}{16\Delta(1 - \Delta)((1 - \Delta)X + \Delta Y)((b - X)(1 - \Delta) + (a - Y)\Delta)}. \quad (3.55)$$

It agrees with the gauge theory result [31].

The corrections terms are determined by the geometric method as usual.

$$\delta_1 = -\frac{(b - X)X(a - Y)Y}{aX + (b - 2X)Y} ((\Delta^1\Delta^7)^2 + (\Delta^4\Delta^6)^2 + (\Delta^2\Delta^8)^2 + (\Delta^3\Delta^5)^2), \quad (3.56)$$

$$\begin{aligned} \delta_2 = & \frac{2(b - X)X(a - Y)Y}{aX + (b - 2X)Y} (\Delta^1\Delta^7\Delta^2\Delta^8 + \Delta^1\Delta^7\Delta^4\Delta^6 + \Delta^2\Delta^8\Delta^3\Delta^5 + \Delta^3\Delta^5\Delta^4\Delta^6) \\ & + \begin{cases} \frac{2(b - X)^2Y^2}{aX + (b - 2X)Y} (\Delta^1\Delta^7\Delta^3\Delta^5 + \Delta^2\Delta^8\Delta^4\Delta^6) & \text{for } aX \leq bY. \\ \frac{2X^2(a - Y)^2}{aX + (b - 2X)Y} (\Delta^1\Delta^7\Delta^3\Delta^5 + \Delta^2\Delta^8\Delta^4\Delta^6) & \text{for } aX > bY. \end{cases} \end{aligned} \quad (3.57)$$

While there are 10 correction terms altogether, the symmetries of the toric diagram leaves only three independent coefficients. Under the general assumptions explained in section 2, the coefficients are uniquely determined. Upon eliminating baryonic charges and imposing the same symmetries for the mesonic charges, we recover the same volume as (3.55).

## 4 Gravity

We turn to the last topic of this paper, namely, the gravity side of the  $\text{AdS}_4/\text{CFT}_3$  correspondence. The geometric free energy discussed earlier is always a quartic polynomial. In this section, we raise the possibility of using the same quartic polynomial as the prepotential in the AdS gauged supergravity. For general toric models, a consistent truncation of the eleven dimensional supergravity is not available. We circumvent the difficulty by focusing on the gauge kinetic terms when the fluctuation of gauge fields are small. Comparing Kaluza-Klein (KK) gravity and gauged supergravity descriptions, we find perfect agreement in the mesonic sector but small discrepancy in the baryonic sector.

### 4.1 Kaluza-Klein supergravity

**M-theory.** Our convention for the bosonic part of the eleven dimensional supergravity is

$$2\kappa_{11}^2 \mathcal{L} = *R - \frac{1}{2}G \wedge *G - \frac{1}{6}C \wedge G \wedge G, \quad (4.1)$$

where  $C$  is the 3-form field and  $G = dC$ . The 11-dimensional Planck length is defined by

$$2\kappa_{11}^2 = (2\pi)^8 l_{11}^9. \quad (4.2)$$

The Einstein equation is given by

$$R_{MN} = \frac{1}{2 \cdot 3!} G_{MPQR} G_N{}^{PQR} - \frac{1}{6} g_{MN} \left( \frac{1}{4!} G_{PQRS} G^{PQRS} \right). \quad (4.3)$$

It admits the vacuum  $\text{AdS}_4 \times Y_7$  solution in the form

$$\bar{ds}^2 = (L/2)^2 ds_{\text{AdS}_4}^2 + L^2 ds_{Y_7}^2, \quad \bar{G} = 3(L/2)^3 \text{vol}_{\text{AdS}_4}, \quad (4.4)$$

where we use the unit normalization for the  $\text{AdS}_4$  and the  $Y_7$  factors,

$$\text{AdS}_4 : R_{\mu\nu} = -3g_{\mu\nu}, \quad Y_7 : R_{\alpha\beta} = 6g_{\alpha\beta}, \quad (4.5)$$

and  $\text{vol}_{\text{AdS}_4}$  denotes the standard volume-form. The flux quantization condition of M-theory determines the radius  $L$  of  $Y$ :

$$\frac{1}{(2\pi l_{11})^6} \int *G = N \implies L^6 = \frac{(2\pi l_{11})^6 N}{6 \text{Vol}(Y)}. \quad (4.6)$$

In what follows, we will abbreviate  $\text{Vol}(Y)$  to  $V$  to simplify equations.

**Baryonic gauge fields.** We follow [22] to normalize the baryon charges by

$$B_a [\Sigma^I] = \frac{2\pi}{V} \int_{\Sigma^I} \omega_a = Q_a^I. \quad (4.7)$$

In other words,  $\{\frac{2\pi}{V}\omega_a\}$  form an integral basis of  $H^5(Y, \mathbb{R})$ . The Kaluza-Klein ansatz for the gauge fields in the baryonic sector is given by

$$G = \bar{G} + 6L^3 (*_4 F^a) \wedge (*_7 \omega_a). \quad (4.8)$$

The normalization of the fluctuation term is fixed by the requirement that the probe M5-branes wrapping the cycles  $\Sigma^I$  are correctly normalized,

$$T_{\text{M5}} \int_{\Sigma^I \times \mathbb{R}_t} \tilde{C}_6 = Q_a{}^I \int_{\mathbb{R}_t} A^a. \quad (4.9)$$

Here,  $\tilde{C}_6$  is the electromagnetic dual form field locally defined by  $d\tilde{C}_6 = *dC_3$ , and  $A^a$  is the gauge field for the field strength in (4.8),  $F^a = dA^a$ . The tension of an M5-brane is  $T_{\text{M5}} = 1/(2\pi)^5 l_{11}^6$ .

At the linearized level, the gauge field satisfy the free field equation,

$$d * F^a = 0 = dF^a, \quad (4.10)$$

and does not mix with metric fluctuations. It is straightforward to compute the gauge kinetic term in the 4-dimensional KK gravity. It is convenient to pull out overall factors of  $L$  and  $\text{Vol}(Y)$ , such that the 4-dimensional Lagrangian is dimensionless.

$$2\kappa_4^2 \mathcal{L}_{\text{KK}} = *(R + 6) - N_{ab} F^a \wedge *F^b + \dots. \quad (4.11)$$

The 4-dimensional metric is unit-normalized as before; it satisfies  $R_{\mu\nu} = -3g_{\mu\nu}$  at the vacuum. The 4-dimensional Newton constant is

$$\frac{1}{2\kappa_4^2} = \frac{L^9 V}{4(2\pi)^8 l_{11}^9} = \frac{\pi}{2} V \left( \frac{N}{V} \right)^{3/2}. \quad (4.12)$$

In this convention, the gauge kinetic term, derived from the 11-dimensional Lagrangian and the KK ansatz, is given by

$$N_{ab} = \frac{9}{V} \int \omega_a \wedge *\omega_b. \quad (4.13)$$

**Mesonic gauge fields.** The correct normalization for the flavor charges is

$$F_i^I = \frac{2\pi}{V} \int_{\Sigma^I} (*dK_i/12) \quad (i = 1, 2, 3, 4). \quad (4.14)$$

As a consistency check, note that

$$\Delta^I = \frac{1}{2} b^i F_i^I = \frac{\pi}{12V} \int_{\Sigma^I} *dK_R = \frac{\pi}{6V} \text{Vol}(\Sigma^I). \quad (4.15)$$

We are abusing the notations a bit and use  $K$  to denote both a Killing vector  $K^\alpha(\partial/\partial x^\alpha)$  and its dual one-form  $g_{\alpha\beta} K^\alpha dx^\beta$ . In the last step of (4.15), we used the local  $U(1)_R$  fibration description of the SE manifold  $Y$ :

$$ds_Y^2 = (e^0)^2 + ds_B^2, \quad e^0 \equiv \frac{1}{4} d\psi + \sigma, \quad K_R = 4 \frac{\partial}{\partial \psi}, \quad (4.16)$$

$$R_{\mu\nu}^{(B)} = 8g_{\mu\nu}^{(B)}, \quad d\sigma = 2J_B, \quad \text{vol}_\Sigma = e^0 \wedge \frac{1}{2} J_B^2. \quad (4.17)$$

The KK ansatz for the mesonic gauge field is slightly involved but well-known. The metric fluctuation takes the standard form; the internal part of the metric is deformed by

$$g_{\alpha\beta}dx^\alpha dx^\beta \rightarrow g_{\alpha\beta}(dx^\alpha + K_i^\alpha A_\mu^i dx^\mu)(dx^\beta + K_j^\beta A_\nu^j dx^\nu). \quad (4.18)$$

This metric fluctuation must be accompanied by a fluctuation of the 4-form flux [37, 38],

$$G = \bar{G} + 2L^3(*F^i) \wedge (dK_i/12). \quad (4.19)$$

The mixing is needed to satisfy the linearized field equation,

$$\nabla^M G_{M\mu\nu\alpha} = \nabla^\beta(\delta G_{\beta\mu\nu\alpha}) - g^{\lambda\sigma}(\delta\Gamma_{\lambda\alpha}^\rho)\bar{G}_{\sigma\mu\nu\rho} = 3\epsilon_{\mu\nu}^{\lambda\sigma}(-F^i + F^i)_{\lambda\sigma}K_{i\alpha} = 0. \quad (4.20)$$

Collecting both contributions, we obtain the kinetic term for the mesonic gauge fields,

$$2\kappa_4^2 \mathcal{L}_{\text{KK}}|_{\text{mesonic}} = -N_{ij}F^i \wedge *F^j, \quad N_{ij} = \frac{2}{V} \int K_i \wedge *K_j. \quad (4.21)$$

## 4.2 Gauged supergravity

We follow the conventions of [39–42] for  $D = 4$ ,  $\mathcal{N} = 2$  gauged supergravity.

**Special geometry.** The vector multiplet part of the  $D = 4$ ,  $\mathcal{N} = 2$  gauged supergravity is governed by the prepotential  $\mathcal{F}$ . It is a homogeneous function of degree two in vector-multiplet scalars  $X^I$ .

$$\mathcal{F}(\lambda X) = \lambda^2 \mathcal{F}(X). \quad (4.22)$$

The derivatives of  $F$  are denoted by

$$\mathcal{F}_I = \partial_I \mathcal{F}, \quad \mathcal{F}_{IJ} \equiv \partial_I \partial_J \mathcal{F}, \quad \mathcal{F}_{IJK} \equiv \partial_I \partial_J \partial_K \mathcal{F}. \quad (4.23)$$

The Kähler potential, the Kähler metric and the Yukawa couplings are given by

$$e^{-K} = i(\bar{X}^I \mathcal{F}_I - X^I \bar{\mathcal{F}}_I) = -2F_{IJ}X^I \bar{X}^J, \quad (4.24)$$

$$e^{-K}g_{i\bar{j}} = e^{-K}\partial_i \partial_{\bar{j}} K = 2D_i X^I D_{\bar{j}} \bar{X}^J F_{IJ}, \quad (4.25)$$

$$C_{ijk} = D_i X^I D_j X^J D_k X^K \mathcal{F}_{IJK}. \quad (4.26)$$

where we defined  $F_{IJ} \equiv \text{Im } \mathcal{F}_{IJ}$ . The following relations hold:

$$F_{IJ}D_i X^J = D_i \mathcal{F}_J, \quad F_{IJ}\bar{X}^I D_i X^J = 0, \quad (4.27)$$

$$\bar{\partial}_i D_j \Omega = g_{i\bar{j}} \Omega, \quad \nabla_i D_j \Omega = i e^K C_{ij}^{\bar{k}} \bar{D}_{\bar{k}} \bar{\Omega}, \quad (4.28)$$

$$R_{i\bar{j}k\bar{l}} = g_{i\bar{j}}g_{k\bar{l}} + g_{i\bar{l}}g_{k\bar{j}} - e^{2K}C_{ik}^{\bar{m}}\bar{C}_{j\bar{l}\bar{m}}. \quad (4.29)$$



**Supergravity Lagrangian.** To write down the vector multiplet part of the  $D = 4$ ,  $\mathcal{N} = 2$  supergravity Lagrangian (see [39–42] for details), we need to introduce

$$\mathcal{N}_{IJ} = \bar{\mathcal{F}}_{IJ} + 2i \frac{F_{IK} X^K F_{JL} X^L}{F_{MN} X^M X^N}, \quad N_{IJ} = -\text{Im} \mathcal{N}_{IJ}, \quad M_{IJ} = \text{Re} \mathcal{N}_{IJ}. \quad (4.30)$$

Some basic properties follow immediately.

$$\mathcal{N}_{IJ} X^J = \mathcal{F}_I, \quad \bar{\mathcal{N}}_{IJ} D_i X^J = D_i \mathcal{F}_I \quad (4.31)$$

$$2 N_{IJ} X^I \bar{X}^J = e^{-K}, \quad 2 N_{IJ} D_i X^I D_{\bar{j}} \bar{X}^J = e^{-K} g_{i\bar{j}}, \quad (4.32)$$

$$N_{IJ} D_i X^I X^J = 0, \quad N^{IJ} = 2e^K (X^I \bar{X}^J + g^{\bar{i}j} D_{\bar{i}} \bar{X}^I D_j X^J). \quad (4.33)$$

The bosonic part of the Lagrangian is

$$\mathcal{L} = *(R - V) - 2g_{i\bar{j}} dt^i \wedge *d\bar{t}^{\bar{j}} - N_{IJ} F^I \wedge \star F^J - M_{IJ} F^I \wedge F^J. \quad (4.34)$$

The scalar potential is determined by some real coefficients  $P_I$ :

$$V = (N^{IJ} - 8e^K X^I \bar{X}^J) P_I P_J = 2e^K \left( g^{\bar{i}j} D_{\bar{i}} \bar{W} D_j W - 3|W|^2 \right), \quad W = P_I X^I. \quad (4.35)$$

The parameters  $P_I$  originate from vacuum expectation values of some hyper-multiplet scalars. Each solution to  $D_i W = 0$  gives a supersymmetric AdS vacuum. We normalize the potential such that  $V|_* = -6$ , which amounts to setting the AdS radius to be unity:  $R_{\mu\nu} = -3g_{\mu\nu}$ . The second derivatives of the potential at the vacuum gives the mass of the scalars. They can be computed using the special geometry relations

$$\bar{\partial}_{\bar{i}} D_j W = g_{i\bar{j}} W, \quad D_i D_j W = ie^K C_{ij}^{\bar{k}} \bar{D}_{\bar{k}} \bar{W} \implies \bar{\partial}_{\bar{i}} \partial_j V|_* = -2g_{i\bar{j}}, \quad \partial_i \partial_j V|_* = 0. \quad (4.36)$$

The mass yields the expected value for the conformal weight of the lowest component of the current superfield:

$$m^2 = \delta(\delta - 3) = -2 \quad \text{or} \quad \delta = 1. \quad (4.37)$$

**Free energy vs prepotential — I.** Our proposal for the prepotential is

$$\mathcal{F} = i\sqrt{\bar{F}^2(X)}. \quad (4.38)$$

with  $\bar{F}^2$  taken from the geometric free energy formula. We further assume that  $\text{Re}(X^I)$  (“axions”) vanishes at the supergravity vacuum and  $\text{Im}(X^I)$  (“dilaton”) is proportional to  $\Delta^I$  of the field theory:

$$X^I = 0 + i\kappa \Delta^I. \quad (4.39)$$

For  $\mathcal{N} = 4$  or higher supersymmetry, this proposal was proposed earlier and verified to reproduce the abelian truncation of the gauged supergravity [43–45]. Let us review the simplest  $\mathcal{N} = 8$  case in which the  $\text{SO}(8)$  gauged supergravity is truncated to its  $\text{U}(1)^4$  subsector. The consistent truncation of this  $\text{U}(1)^4$  supergravity from the eleven dimensional

supergravity was performed in [46]. For simplicity, we focus on the axion-free sector. The reduction ansatz for the metric is

$$ds_{11}^2 = H^{2/3} ds_4^2 + 4H^{-1/3} \sum_I X_i^{-1} (d\phi^i + \mu_i^2 A^i/2)^2, \quad H = \sum_{i=1}^4 X_i \mu_i^2, \quad \sum_i \mu_i^2 = 1, \quad (4.40)$$

where we used a normalization equivalent to  $L = 2$  in (4.4). The reduction ansatz for the 4-form field strength can be found in [46]. It is convenient to parametrize the scalars  $X_i$ , which satisfy  $X_1 X_2 X_3 X_4 = 1$ , with three scalars  $\vec{\varphi} = (\varphi_1, \varphi_2, \varphi_3)$  as  $X_i = e^{-\frac{1}{2} \vec{a}_i \cdot \vec{\varphi}}$ , where

$$\vec{a}_1 = (1, 1, 1), \quad \vec{a}_2 = (1, -1, -1), \quad \vec{a}_3 = (-1, 1, -1), \quad \vec{a}_4 = (-1, -1, 1). \quad (4.41)$$

Then the resulting four dimensional supergravity Lagrangian reads

$$\begin{aligned} \mathcal{L} &= *(R - V) - \frac{1}{2} (\partial \vec{\varphi})^2 - \frac{1}{2} \sum_{i=1}^4 e^{\vec{a}_i \cdot \vec{\varphi}} F_i \wedge *F_i, \\ V &= -2(\cos \varphi_1 + \cos \varphi_2 + \cos \varphi_3). \end{aligned} \quad (4.42)$$

Clearly, the vacuum of this potential is at  $\vec{\varphi} = 0$  or  $X_i = 1$ .

In [44], it was shown that the prepotential  $\mathcal{F} = i\sqrt{X_1 X_2 X_3 X_4}$  with the gauge choice  $X_1 X_2 X_3 X_4 = 1$  and the recipe to derive the bosonic Lagrangian (4.34) exactly reproduces the Lagrangian (4.42). The agreement between the consistent truncation and the gauged supergravity continues to hold even if the axions are turned on. The comparison was also extended to the abelian truncation of  $\mathcal{N} = 4$  orbifold theories and perfect agreement was found.

**Free energy vs prepotential — II.** Guided by the success for  $\mathcal{N} \geq 4$  theories, we test the proposal (4.38) for general  $\mathcal{N} = 2$  toric models. If we focus on the computation of the gauge kinetic terms  $N_{IJ}$  at the vacuum, we can use the following simplified formula,

$$N_{IJ} = \frac{1}{2} \left( \frac{\partial_I \partial_J (F^2)}{(F^2)^{1/2}} - \frac{\partial_I (F^2) \partial_J (F^2)}{(F^2)^{3/2}} \right). \quad (4.43)$$

The derivation of this formula goes as follows. We will take  $X^I$  to be purely imaginary from the beginning, but will leave  $\text{Im} X^I$  undetermined until the very end.

$$\begin{aligned} \mathcal{F} &= i\sqrt{F^2(X)}, \quad F^2(X) = \frac{1}{24} C_{IJKL} X^I X^J X^K X^L, \\ \mathcal{F}_{IJ} &= i\partial_I \left( \frac{\partial_J (F^2)}{2(F^2)^{1/2}} \right) = i \left( \frac{1}{2} \frac{\partial_I \partial_J (F^2)}{(F^2)^{1/2}} - \frac{1}{4} \frac{\partial_I (F^2) \partial_J (F^2)}{(F^2)^{3/2}} \right) = iF_{IJ}, \\ \mathcal{N}_{IJ} &= \bar{\mathcal{F}}_{IJ} + 2i \frac{F_{IK} X^K F_{JL} X^L}{F_{MN} X^M X^N} = -i \left( F_{IJ} - 2 \frac{F_{IK} X^K F_{JL} X^L}{F_{MN} X^M X^N} \right) = -iN_{IJ}. \end{aligned} \quad (4.44)$$

So far, we have used reality conditions only. We can simplify the formula further using the homogeneity of  $F^2$ .

$$\begin{aligned}
F_{IK}X^K &= \frac{1}{2} \frac{X^K \partial_K (\partial_I (F^2))}{(F^2)^{1/2}} - \frac{1}{4} \frac{\partial_I (F^2) X^K \partial_K (F^2)}{(F^2)^{3/2}} \\
&= \frac{3}{2} \frac{\partial_I (F^2)}{(F^2)^{1/2}} - \frac{\partial_I (F^2)}{(F^2)^{1/2}} = \frac{1}{2} \frac{\partial_I (F^2)}{(F^2)^{1/2}}, \\
F_{MN}X^M X^N &= \frac{1}{2} \frac{X^M \partial_M (F^2)}{(F^2)^{1/2}} = 2(F^2)^{1/2}.
\end{aligned} \tag{4.45}$$

Inserting (4.45) into (4.44), we arrive at (4.43).

Let us proceed to examine the value of  $N_{IJ}$  at the vacuum. To compare the result with those of KK supergravity, we decompose the gauge kinetic coefficients into the baryonic, mesonic, and the R-symmetry directions. In the notations of section 2,

$$N_{ij} = F_i^I F_j^J N_{IJ}, \quad N_{ab} = Q_a^I Q_b^J N_{IJ}. \tag{4.46}$$

A straightforward computation shows that

$$\begin{aligned}
N_{ab} &= \left. \frac{m_{ab}}{2(F^2)^{1/2}} \right|_*, & N_{Ra} &= 0, & N_{ia} &= 0, \\
N_{ij} &= \left. \frac{\partial_i \partial_j F^2}{2(F^2)^{1/2}} \right|_*, & N_{Ri} &= 0, & N_{RR} &= \frac{1}{2}.
\end{aligned} \tag{4.47}$$

Here  $m_{ab}$  is the quadratic function introduces in (2.27). The decoupling of the R-symmetry component from all others is as expected [37]. The mesonic coefficients  $N_{ij}$  matches precisely with those obtained from the KK supergravity (4.21) as can be proved by identities for toric geometry [18]. As for the baryonic ones, we do not have general formula to relate  $m_{ab}$  and the KK formula (2.27). However, in all examples we have tested, the two results differ by an overall constant.

$$N_{ab}(\text{KK}) = \frac{3}{4} N_{ab}(\text{prepotential}). \tag{4.48}$$

This discrepancy does not lead to an immediate contradiction. Our proposal for the prepotential was carried over from previous work for  $\mathcal{N} \geq 4$  theories, but there was no a priori reason for its validity for general  $\mathcal{N} = 2$  theories. It would be still desirable to gain further insight on the close resemblance between the free energy and the prepotential. Since the free energy is obtained by a localization computation on the CFT<sub>3</sub> side, it might be a good to apply the localization technique in the AdS<sub>4</sub> supergravity. In a recent work [47], a localization computation for supergravity was performed for  $\mathcal{N} \geq 3$  AdS<sub>4</sub>/CFT<sub>3</sub> models, which made use of a square-root prepotential originally proposed in [48]. It would be interesting to apply the ideas of [47] to the toric models considered in this paper.

## Acknowledgments

SL thanks Seok Kim and Sungjay Lee for collaborations on a closely related unpublished work in 2007–2008, and Kevin Goldstein, Yuji Tachikawa, and Sandip Trivedi for helpful

discussions over the same period. We thank Raju Roychowdhury for collaboration at an early stage of this work. This work was supported in part by the National Research Foundation of Korea (NRF) Grants 2012R1A1B3001085 and 2012R1A2A2A02046739. The work of DY is supported in part by Perimeter Institute for Theoretical Physics. Research at Perimeter Institute is supported by the Government of Canada through Industry Canada and by the Province of Ontario through the Ministry of Economic Development and Innovation.

**Open Access.** This article is distributed under the terms of the Creative Commons Attribution License ([CC-BY 4.0](https://creativecommons.org/licenses/by/4.0/)), which permits any use, distribution and reproduction in any medium, provided the original author(s) and source are credited.

## References

- [1] A. Hanany and K.D. Kennaway, *Dimer models and toric diagrams*, [hep-th/0503149](#) [[INSPIRE](#)].
- [2] S. Franco, A. Hanany, K.D. Kennaway, D. Vegh and B. Wecht, *Brane dimers and quiver gauge theories*, *JHEP* **01** (2006) 096 [[hep-th/0504110](#)] [[INSPIRE](#)].
- [3] S. Lee, *Superconformal field theories from crystal lattices*, *Phys. Rev. D* **75** (2007) 101901 [[hep-th/0610204](#)] [[INSPIRE](#)].
- [4] S. Lee, S. Lee and J. Park, *Toric  $AdS_4/CFT_3$  duals and M-theory crystals*, *JHEP* **05** (2007) 004 [[hep-th/0702120](#)] [[INSPIRE](#)].
- [5] S. Kim, S. Lee, S. Lee and J. Park, *Abelian gauge theory on M2-brane and toric duality*, *Nucl. Phys. B* **797** (2008) 340 [[arXiv:0705.3540](#)] [[INSPIRE](#)].
- [6] D. Martelli and J. Sparks, *Notes on toric Sasaki-Einstein seven-manifolds and  $AdS_4/CFT_3$* , *JHEP* **11** (2008) 016 [[arXiv:0808.0904](#)] [[INSPIRE](#)].
- [7] D. Martelli and J. Sparks, *Moduli spaces of Chern-Simons quiver gauge theories and  $AdS_4/CFT_3$* , *Phys. Rev. D* **78** (2008) 126005 [[arXiv:0808.0912](#)] [[INSPIRE](#)].
- [8] A. Hanany and A. Zaffaroni, *Tilings, Chern-Simons theories and M2 branes*, *JHEP* **10** (2008) 111 [[arXiv:0808.1244](#)] [[INSPIRE](#)].
- [9] K. Ueda and M. Yamazaki, *Toric Calabi-Yau four-folds dual to Chern-Simons-matter theories*, *JHEP* **12** (2008) 045 [[arXiv:0808.3768](#)] [[INSPIRE](#)].
- [10] Y. Imamura and K. Kimura, *Quiver Chern-Simons theories and crystals*, *JHEP* **10** (2008) 114 [[arXiv:0808.4155](#)] [[INSPIRE](#)].
- [11] A. Hanany, D. Vegh and A. Zaffaroni, *Brane tilings and M2 branes*, *JHEP* **03** (2009) 012 [[arXiv:0809.1440](#)] [[INSPIRE](#)].
- [12] S. Franco, A. Hanany, J. Park and D. Rodriguez-Gómez, *Towards M2-brane theories for generic toric singularities*, *JHEP* **12** (2008) 110 [[arXiv:0809.3237](#)] [[INSPIRE](#)].
- [13] M. Aganagic, *A stringy origin of M2 brane Chern-Simons theories*, *Nucl. Phys. B* **835** (2010) 1 [[arXiv:0905.3415](#)] [[INSPIRE](#)].
- [14] F. Benini, C. Closset and S. Cremonesi, *Chiral flavors and M2-branes at toric CY4 singularities*, *JHEP* **02** (2010) 036 [[arXiv:0911.4127](#)] [[INSPIRE](#)].

- [15] F. Benini, C. Closset and S. Cremonesi, *Quantum moduli space of Chern-Simons quivers, wrapped D6-branes and  $AdS_4/CFT_3$* , *JHEP* **09** (2011) 005 [[arXiv:1105.2299](#)] [[INSPIRE](#)].
- [16] C. Closset and S. Cremonesi, *Toric Fano varieties and Chern-Simons quivers*, *JHEP* **05** (2012) 060 [[arXiv:1201.2431](#)] [[INSPIRE](#)].
- [17] K.A. Intriligator and B. Wecht, *The exact superconformal  $R$  symmetry maximizes  $a$* , *Nucl. Phys. B* **667** (2003) 183 [[hep-th/0304128](#)] [[INSPIRE](#)].
- [18] D. Martelli, J. Sparks and S.-T. Yau, *The geometric dual of  $a$ -maximisation for toric Sasaki-Einstein manifolds*, *Commun. Math. Phys.* **268** (2006) 39 [[hep-th/0503183](#)] [[INSPIRE](#)].
- [19] D. Martelli, J. Sparks and S.-T. Yau, *Sasaki-Einstein manifolds and volume minimisation*, *Commun. Math. Phys.* **280** (2008) 611 [[hep-th/0603021](#)] [[INSPIRE](#)].
- [20] A. Butti and A. Zaffaroni,  *$R$ -charges from toric diagrams and the equivalence of  $a$ -maximization and  $Z$ -minimization*, *JHEP* **11** (2005) 019 [[hep-th/0506232](#)] [[INSPIRE](#)].
- [21] A. Butti and A. Zaffaroni, *From toric geometry to quiver gauge theory: the equivalence of  $a$ -maximization and  $Z$ -minimization*, *Fortsch. Phys.* **54** (2006) 309 [[hep-th/0512240](#)] [[INSPIRE](#)].
- [22] S. Benvenuti, L.A. Pando Zayas and Y. Tachikawa, *Triangle anomalies from Einstein manifolds*, *Adv. Theor. Math. Phys.* **10** (2006) 395 [[hep-th/0601054](#)] [[INSPIRE](#)].
- [23] S. Lee and S.-J. Rey, *Comments on anomalies and charges of toric-quiver duals*, *JHEP* **03** (2006) 068 [[hep-th/0601223](#)] [[INSPIRE](#)].
- [24] A. Kapustin, B. Willett and I. Yaakov, *Exact results for Wilson loops in superconformal Chern-Simons theories with matter*, *JHEP* **03** (2010) 089 [[arXiv:0909.4559](#)] [[INSPIRE](#)].
- [25] D.L. Jafferis, *The exact superconformal  $R$ -symmetry extremizes  $Z$* , *JHEP* **05** (2012) 159 [[arXiv:1012.3210](#)] [[INSPIRE](#)].
- [26] N. Hama, K. Hosomichi and S. Lee, *Notes on SUSY gauge theories on three-sphere*, *JHEP* **03** (2011) 127 [[arXiv:1012.3512](#)] [[INSPIRE](#)].
- [27] C. Closset, T.T. Dumitrescu, G. Festuccia, Z. Komargodski and N. Seiberg, *Contact terms, unitarity and  $F$ -maximization in three-dimensional superconformal theories*, *JHEP* **10** (2012) 053 [[arXiv:1205.4142](#)] [[INSPIRE](#)].
- [28] D. Martelli and J. Sparks, *The large- $N$  limit of quiver matrix models and Sasaki-Einstein manifolds*, *Phys. Rev. D* **84** (2011) 046008 [[arXiv:1102.5289](#)] [[INSPIRE](#)].
- [29] S. Cheon, H. Kim and N. Kim, *Calculating the partition function of  $N = 2$  gauge theories on  $S^3$  and  $AdS/CFT$  correspondence*, *JHEP* **05** (2011) 134 [[arXiv:1102.5565](#)] [[INSPIRE](#)].
- [30] D.L. Jafferis, I.R. Klebanov, S.S. Pufu and B.R. Safdi, *Towards the  $F$ -theorem:  $N = 2$  field theories on the three-sphere*, *JHEP* **06** (2011) 102 [[arXiv:1103.1181](#)] [[INSPIRE](#)].
- [31] A. Amariti and S. Franco, *Free energy vs. Sasaki-Einstein volume for infinite families of  $M2$ -brane theories*, *JHEP* **09** (2012) 034 [[arXiv:1204.6040](#)] [[INSPIRE](#)].
- [32] A. Amariti, C. Klare and M. Siani, *The large- $N$  limit of toric Chern-Simons matter theories and their duals*, *JHEP* **10** (2012) 019 [[arXiv:1111.1723](#)] [[INSPIRE](#)].
- [33] S. Franco et al., *Gauge theories from toric geometry and brane tilings*, *JHEP* **01** (2006) 128 [[hep-th/0505211](#)] [[INSPIRE](#)].

- [34] D. Berenstein, C.P. Herzog and I.R. Klebanov, *Baryon spectra and AdS/CFT correspondence*, *JHEP* **06** (2002) 047 [[hep-th/0202150](#)] [[INSPIRE](#)].
- [35] O. Aharony, O. Bergman, D.L. Jafferis and J. Maldacena,  *$N = 6$  superconformal Chern-Simons-matter theories, M2-branes and their gravity duals*, *JHEP* **10** (2008) 091 [[arXiv:0806.1218](#)] [[INSPIRE](#)].
- [36] C.P. Herzog, I.R. Klebanov, S.S. Pufu and T. Tesileanu, *Multi-matrix models and tri-Sasaki Einstein spaces*, *Phys. Rev. D* **83** (2011) 046001 [[arXiv:1011.5487](#)] [[INSPIRE](#)].
- [37] E. Barnes, E. Gorbatov, K.A. Intriligator, M. Sudano and J. Wright, *The exact superconformal R-symmetry minimizes  $\tau_{RR}$* , *Nucl. Phys. B* **730** (2005) 210 [[hep-th/0507137](#)] [[INSPIRE](#)].
- [38] E. Barnes, E. Gorbatov, K.A. Intriligator and J. Wright, *Current correlators and AdS/CFT geometry*, *Nucl. Phys. B* **732** (2006) 89 [[hep-th/0507146](#)] [[INSPIRE](#)].
- [39] B. de Wit and A. Van Proeyen, *Potentials and symmetries of general gauged  $N = 2$  supergravity: Yang-Mills models*, *Nucl. Phys. B* **245** (1984) 89 [[INSPIRE](#)].
- [40] L. Andrianopoli et al., *General matter coupled  $N = 2$  supergravity*, *Nucl. Phys. B* **476** (1996) 397 [[hep-th/9603004](#)] [[INSPIRE](#)].
- [41] B. Craps, F. Roose, W. Troost and A. Van Proeyen, *What is special Kähler geometry?*, *Nucl. Phys. B* **503** (1997) 565 [[hep-th/9703082](#)] [[INSPIRE](#)].
- [42] J. Louis and A. Micu, *Type 2 theories compactified on Calabi-Yau threefolds in the presence of background fluxes*, *Nucl. Phys. B* **635** (2002) 395 [[hep-th/0202168](#)] [[INSPIRE](#)].
- [43] S. Lee, *Prepotentials in toric  $AdS_4$  compactifications*, *Int. J. Mod. Phys. A* **23** (2008) 2197 [[INSPIRE](#)].
- [44] S. Lee, *Studies on three dimensional superconformal theories and their gravity duals*, Ph.D. thesis, Seoul National University, Seoul, South Korea (2008), see chapter 4.
- [45] S. Kim, S. Lee and S. Lee, unpublished.
- [46] M. Cvetič et al., *Embedding AdS black holes in ten-dimensions and eleven-dimensions*, *Nucl. Phys. B* **558** (1999) 96 [[hep-th/9903214](#)] [[INSPIRE](#)].
- [47] A. Dabholkar, N. Drukker and J. Gomes, *Localization in supergravity and quantum  $AdS_4/CFT_3$  holography*, *JHEP* **1410** (2014) 90 [[arXiv:1406.0505](#)] [[INSPIRE](#)].
- [48] J.P. Gauntlett, S. Kim, O. Varela and D. Waldram, *Consistent supersymmetric Kaluza-Klein truncations with massive modes*, *JHEP* **04** (2009) 102 [[arXiv:0901.0676](#)] [[INSPIRE](#)].